The Doublesex-related Dmrta2 safeguards neural progenitor maintenance involving transcriptional regulation of Hes1

Fraser I. Young[1], Marc Keruzore[2#], Xinsheng Nan[3,#], Nicole Gennet[1], Eric J. Bellefroid[2‡], Meng Li[1,3‡]

1, Neuroscience and Mental Health Research Institute, School of Medicine, Cardiff University, Cardiff, CF24 4HQ, UK

2, ULB Institute of Neuroscience (UNI), Université Libre de Bruxelles (ULB), B-6041 Gosselies, Belgium

3, School of Bioscience, Cardiff University, Cardiff, CF24 4HQ, UK

[#] These authors contributed equally

[‡]**Corresponding authors:**

Meng Li, email: LiM26@cardiff.ac.uk Tel: +44 29206 88345

Eric Bellefroid, email: ebellefr@ulb.ac.be Tel: +32 26509732

Short Title: Dmrta2 controls neural progenitor maintenance

KEY WORDS: Dmrta2, Hes1, cell cycle, transcription factor, neurogenesis,

Significance

Maintaining an intricate balance between continued progenitor proliferation and cell cycle exit/differentiation is pivotal for proper brain development. Disruption of this delicate process can lead to brain malformations such as microlissencephaly. The current work identifies Dmrta2 as an important transcription factor that helps to regulate the fine tuning between cell cycle progression and neuronal differentiation. Mechanistically, this function of Dmrta2 involves direct transcriptional regulation of a known repressor of neurogenesis Hes1. Our findings thus add Dmrta2 to the complex regulatory machinery controlling cortical NPC maintenance, and provide an explanation to the microlissencephaly caused by Dmrta2-deficiency in model organisms and man.

Abstract

The mechanisms that determine whether a neural progenitor cell (NPC) re-enters the cell cycle or exits and differentiates are pivotal for generating cells in correct numbers and diverse types, and hence dictate proper brain development. Combining gain-of-function and loss-of-function approaches in an embryonic stem cell-derived cortical differentiation model, we report that Dmrta2 plays an important role in maintaining NPCs in the cell cycle. Temporally controlled expression of transgenic *Dmrta2* in NPCs suppresses differentiation without affecting their neurogenic competence. In contrast, *Dmrta2* knockout accelerates the cell cycle exit and differentiation into post-mitotic neurons of NPCs derived from embryonic stem cells and in Emx1-cre conditional mutant mice. Dmrta2 function was linked to the regulation of *Hes1* and other proneural genes as demonstrated by genome wide RNAseq and direct binding of Dmrta2 to the *Hes1* genomic locus. Moreover, transient *Hes1* expression rescues precocious neurogenesis in *Dmrta2* knockout NPCs. Our study therefore establishes a novel link between Dmrta2 modulation of *Hes1* expression and the maintenance of NPCs during cortical development.

Introduction

Balancing neural progenitor cell (NPC) self-renewal and neuronal differentiation is essential for generating cells in correct numbers and diverse types during brain development (1, 2). As such, cortical neurogenesis is tightly regulated by a complex array of transcription factors that work in concert to coordinate NPC maintenance and differentiation. Proneural transcription factors, such as neurogenin (Neurog) and Neurod, act as the primary initiators of differentiation through their direct regulation of target genes associated with cytoskeletal reorganisation, migration and other critical differentiation processes (3, 4). Proneural transcription factors are themselves subject to transcriptional regulation by other cortical transcription factors such as Pax6 and Hes1. Pax6 acts upstream to promote neuronal differentiation through its direct activation of proneural genes (5). On the other hand, the basic helix-loop-helix transcription factor Hes1 promotes NPC proliferation and self-renewal through its repressive actions on proneural gene expression, thereby restricting spontaneous differentiation (6). Significant disruptions to this delicate regulatory network can result in severe developmental defects due to altered neuronal production (1, 2). One such disorder is microlissencephaly, a rare genetic-linked group of neurodevelopmental malformations characterised by the absence of sulci and gyri of the cerebral cortex and an accompanying reduction in cortical size and volume. Recently, a loss-of-function mutation in the Doublesex- and Mab-3-related transcription factor A2 (*DMRTA2*, also known as *DMRT5*) gene has been reported in a case of microlissencephaly, implicating *DMRTA2* as a critical regulator of cortical NPC dynamics (7).

Dmrta2 belongs to the highly conserved family of *Dmrt* transcription factors whose roles in the developing reproductive system have been extensively characterised (8). However, a further site of expression and function of *Dmrta2* has been found in the embryonic brain (9, 10). *Dmrta2* loss-of-function in Zebrafish leads to significant reductions in cortical size, coupled with reduced neuronal numbers (10, 11). Likewise, a smaller neocortex, particularly dorsomedial neocortex, has been observed in mice carrying null deletions of *Dmrta2* (12-14). Together with the association of *DMRTA2* mutation and microlissencephaly in humans, these findings implicate *Dmrta2* as an important regulator for cortical neurogenesis. However, *Dmrta2*-null mice additionally present agenesis of the embryonic cortical hem. The cortical hem is the embryonic organizer for the hippocampus and a major regulator of cortical patterning outside the hippocampus. It provides a source of Wingless-related (WNT) and bone morphogenetic protein (BMP) signalling in the dorsomedial telencephalon to control proper cortical regionalisation and NPC expansion in a paracrine fashion (15, 16). Thus, the severe patterning and arealisation defects in *Dmrta2*-null model organisms prohibit a clear dissection between a direct role of *Dmrta2* in NPC behaviour from the secondary effect of an overall reduction in extrinsic hem-derived signals. More recently, conditional *Dmrta2* mutant mice (*Dmrta2*$^{fl/fl}$*;Emx1-cre*), that delete *Dmrta2* in cortical progenitors after cortical hem formation, also have reduced cortical hemisphere size suggesting a direct role of Dmrta2 in the control of NPC behaviour, which remains to be defined (14).

Embryonic stem cells (ESCs) are capable of giving rise to all somatic cell types with easy access during *in vitro* differentiation. Mouse and human ESCs can efficiently generate cortical NPCs in culture without any added morphogens and subsequently differentiated into layer-specific neurons in a temporally regulated fashion recapitulating major steps of normal cortical development (17-19). In this study, we analysed the behaviour of mouse ESC-derived cortical progenitors either lacking *Dmrta2* or conditionally expressing transgenic *Dmrta2* (9). We report that enforced expression of *Dmrta2* in cortical NPCs suppresses neuronal differentiation without affecting neurogenic competence, while in its absence cortical NPCs undergo precocious cell cycle exit and neuronal differentiation *in vitro* and *in*

vivo. We provide evidence that Dmrta2 maintains NPC status via transcriptional regulation of *Hes1*. Thus, this study identifies a new layer of genetic control by *Dmrta2* in fine tuning cortical NPC proliferation and terminal differentiation.

Results

Expression of *Dmrta2* by ESC-derived cortical NPCs

In order to achieve efficient induction of cortical fate from mouse ESCs, we incorporated in our protocol several measures previously shown to promote a dorsal telencephalic fate (Fig. 1*A*) (17). These included dual SMAD inhibition with SB431542 and LDN193189 to accelerate neural induction (20), the addition of a Wnt inhibitor XAV to suppress caudalization (21, 22), and cyclopamine to antagonise ventralisation of neural progenitor cells by endogenous sonic hedgehog (SHH) signalling (cultures generated by this paradigm are referred to hereafter as cortical cultures) (18). As negative controls for cortical identity, we in parallel induced ESCs towards a ventral telencephalic fate with SHH, a caudal fate with retinoic acid, and a ventral mesencephalic (dopaminergic) fate using a combinatorial treatment of ERK inhibitor and SHH (Fig S1*A*) (23). The generation of cortical NPCs was verified by immunostaining at day 6-8 for cortical specific or cortical enriched markers Pax6, Lmx1a, Eomes (Tbr2), Otx2, Coup-TF1 and FORSE-1 (also known as LeX) along with nestin as a pan NPC marker (Fig. 1*B* and *C*, Fig. S1*B* and *D*). The vast majority of cells in the cortical cultures stained positive for Pax6, FORSE-1, Otx2, Lmx1a, Coup-TF1 and nestin, while a proportion of cells also expressed Eomes. The transcription factor Nkx2.1 is specifically expressed by medial ganglionic eminence progenitors. While abundant Nkx2.1$^+$ cells were detected in SHH treated ventral telencephalic cultures, negligible numbers of Nkx2.1$^+$ cells were found in cortical cultures (Fig. S1*B*). Foxa2 is a marker for the ventral midbrain and spinal cord. Few Foxa2$^+$ cells were observed in the cortical cultures while they constituted the major population in dopaminergic differentiated cultures (Fig. S1*C*).

Double immunocytochemistry showed that Dmrta2$^+$ cells were confined to Nestin$^+$ and FORSE-1$^+$ NPCs in cortical cultures, representing 30-54% of the total cell population between day 4-10 (Fig. 1*B* and *D*). During development, *Dmrta2* expression is restricted to the dorsal telencephalon where it is co-expressed with *Pax6* but in an opposite gradient (12, 13, 24). Consistent with its expression *in vivo*, we found that Dmrta2 and Pax6 staining largely overlapped in ESC-derived NPCs localized in neural rosettes, from which Eomes$^+$ basal progenitor cells could be seen extending distally (Fig. 1*C*). In contrast, no Dmrta2$^+$ cells were found in SHH- or retinoic acid- treated neural progenitor cultures (Fig S1*B* and *D*).

Dmrta2$^+$ cells were no longer detectable by day 15 of differentiation. At this stage, the presence of postmitotic cortical neurons was confirmed by immunostaining for cortical layer-specific neuronal markers Tbr1 (layer VI), Bcl11b (Ctip2 (layer V and VI)), and Satb2 (layer II/III) and a pan-glutamatergic neuronal marker vGlut1 (Fig. 1*E* and *F*, Fig. S1*E*). Very few GABAergic neurons, identified by GAD65/67 immunostaining, were observed in the cortical cultures (Fig. S1*E*). Moreover, we did not observe TH$^+$/Nurr1$^+$ dopaminergic neurons or Isl1$^+$/Olig2$^+$ spinal motor neurons, confirming an enrichment of cortical neurons in our cultures (Fig S1*F* and *G*). Together, our data demonstrates the ability to reproduce *in vitro* Dmrta2$^+$ dorsal telencephalic NPCs and their neuronal progeny.

Enforced expression of Dmrta2 suppresses NPC neuronal differentiation

To investigate a role for Dmrta2 in telencephalic NPC behaviour, we firstly examined the effect of Dmrta2 gain of function in neuronal differentiation of ESC-derived NPCs using a tetracycline-inducible *Dmrta2* transgenic mESC model (*Dmrta2*-ESCs) reported previously (9). These cells harbour the reverse tetracycline-controlled transactivator (rtTA) and produce significant levels of Dmrta2 protein in response to the addition of doxycycline to the culture

media. *Dmrta2* transgene was induced at the peak of NPC production for 7 days from day 5 and the expression of several neurogenic genes examined by qPCR (Fig. 2*A* and *B*). In the control condition, without doxycycline, the level of proneural gene transcripts (*Neurog2*, *Neurod1* and *Neurod4*) increased gradually from day 6, along with the immature neuronal marker gene *Tubb3* (β3-tubulin). However, lower levels of all these transcripts were detected in parallel sister cultures treated with doxycycline at all timepoints analysed. In contrast, the transcript levels of *Hes1*, a repressor of cortical neurogenesis, was robustly upregulated (Fig. 2*B*). These gene expression changes were concurrent with the induced transgenic *Dmrta2* from day 6, which remained at a higher level than in control cultures throughout.

Consistent with the qPCR observations, cells exposed to doxycycline for 5 days maintained a largely NPC morphology while the sister control cells progressed to terminal differentiation into neurons (Fig. 2*C*). Immunostaining confirmed a marked reduction of $Tubb3^+$ cells in doxycycline treated cultures compared to controls. In contrast, doxycycline-treated cultures contained more $Nestin^+$ NPCs (Fig. 2*D*). Moreover, double immunocytochemistry for Dmrta2 and Tubb3 revealed mutually exclusive staining in doxycycline-treated cultures, providing direct evidence that a high level of Dmrta2 suppresses neuronal differentiation of NPCs (Fig. 2*E*).

Interestingly, upon removal of doxycycline after 4 days treatment, the NPCs readily gave rise to $Tubb3^+$ neurons (Fig. S2). This finding suggests that a high level of Dmrta2 favours NPC maintenance over neuronal differentiation without affecting their neurogenic competence.

Loss of Dmrta2 accelerates neuronal differentiation of cortical NPCs

To gain further insights into the physiological function of Dmrta2 in neurogenesis and the cellular mechanisms that might underpin microcephaly caused by Dmrta2 loss-of-function mutation, we generated lines of mESCs with homozygous deletion of *Dmrta2* (*Dmrta2*$^{-/-}$) by gene targeting and directed these cells towards cortical fate (Fig. 3 and Fig. S3). We closely monitored neural induction and neuronal differentiation in *Dmrta2*$^{-/-}$ and isogenic control (*Dmrta2*$^{flox/flox}$) cultures by immunocytochemistry and qPCR (Fig. 3*A* and *B*). Rapid neuroepithelial fate conversion was observed in both genotypes as demonstrated by the generation of a similar proportion of $Nestin^+$ NPCs at day 4 and day 6 (Fig. 3*A*). However, following the onset of *Dmrta2* expression at day 4, we observed marked differences in the temporal expression profile of the intermediate progenitor marker gene *Eomes*, neuronal marker *Map2*, and proneural transcription factors *Neurog2* and *Neurod1* (Fig. 3*B*). *Map2* and *Eomes* levels were increased in the *Dmrta2*$^{-/-}$ cultures while both *Neurog2* and *Neurod1* RNA reached their highest levels sooner in *Dmrta2*$^{-/-}$ cells than the control cells, suggesting an early initiation of neurogenesis programme. Consistent with this observation, we detected an increase in the production of $Tubb3^+$ neurons in *Dmrta2*$^{-/-}$ cultures by immunostaining at days 4, 6 and 8 compared to the isogenic control cultures (Fig. 3*C*). Similarly, *Dmrta2*$^{-/-}$ cultures also contained significantly more $NeuN^+$ cells (mature neurons) at days 10 to 14 (Fig. 3*D*).

In the reduced cortex of *Dmrta2*$^{-/-}$ embryos, a transient increase in neuronal production has also been observed during early corticogenesis. This excess of neuronal production during early neurogenesis may be a secondary consequence of the reduction of Wnt cortical hem signals or a direct consequence of the loss of *Dmrta2* in cortical progenitors (12). To test this latter possibility, we assessed by immunostaining the amount of $Tubb3^+$ and $Eomes^+$ cells in the cortical plate of E11 conditional *Dmrta2* mutant mice (*Dmrta2*$^{fl/fl}$*;Emx1-cre*) in which Wnt signalling pathway appears unaffected (14). An increase of $Tubb3^+$ and of $Eomes^+$ cells was found in the conditional *Dmrta2* mutant mice relative to controls (Fig. 4). Thus, premature neuronal differentiation is also a feature *in vivo* of conditional *Dmrta2* mutant mice,

corroborating the *in vitro* observations and suggesting a direct role for Dmrta2 in cortical NPC neurogenesis.

Altered Dmrta2 levels leads to cell cycle dysregulation in cortical NPCs

Disrupted cortical NPC proliferation and cell cycle progression has been implicated as an underlying mechanism for microlissencephaly (25). To determine whether Dmrta2 plays a role in cell cycle regulation, we performed a flow cytometry-based cell cycle analysis to reveal the distribution of Nestin^{+} NPCs in three major phases of the cell cycle (G0/1, S and G2/M) (Fig. 5*A*). Significantly more *Dmrta2*$^{-/-}$ cortical NPCs were found in G0/1 phase ($p<0.01$) than the control cells at day 6 of differentiation (Fig. 5*B*). Accordingly, the number of cells in the S phase was reduced ($p<0.05$) in day 6 *Dmrta2*$^{-/-}$ NPCs compared to controls, although no differences were found on days 8 and 10.

To gain further insight into Dmrta2-regulated cell cycle progression, we carried out EdU incorporation assays at days 6, 8 and 10 of differentiation. This study revealed a reduction in the number of EdU-labelled cells in *Dmrta2*$^{-/-}$ cultures compared to control cultures at all three time points, providing independent evidence of altered S phase in *Dmrta2*$^{-/-}$ NPCs (Fig. 5*C*). Moreover, immunocytochemical analysis showed that cells expressing Cdkn1b (p27kip1) and Cdkn1c (p57Kip2) are both increased in *Dmrta2*$^{-/-}$ cultures compared to controls (Fig. 5*C*). Cdkn1b and Cdkn1c are cell cycle regulators with a major function to halt or slow the G1-S phase transition and hence their upregulation is closely associated with cell cycle exit and neuronal differentiation. In contrast, we observed a reduction at the transcript level of these two cell cycle regulators and an increase in the proportion of Ki67^{+} cells when NPCs were forced to express Dmrta2 (Fig. S4). Together, these findings identify a new role for Dmrta2 in NPC cell cycle regulation and suggest that the disrupted regulation of cell cycle progression in *Dmrta2*$^{-/-}$ NPCs may be a significant contributory factor to the precocious neurogenesis described above.

Genome-wide transcriptome profiling supports a role for Dmrta2 in NPC neurogenesis

In order to gain insight into the molecular mechanisms underlying the altered neurogenesis in *Dmrta2*-deficient NPCs, we carried out a transcriptome analysis by RNA sequencing (RNAseq) using day 8 cultures, a timepoint associated with the highest number of Dmrta2^{+} cells and when both neurogenic and proliferative defects were apparent. Analysis of this RNAseq dataset identified 7343 differentially expressed transcripts at a significance level of $p<0.05$ (Fig. 6*A*, Fig. S5 and Dataset S1). Amongst the *Dmrta2*-regulated genes were a number of transcription factors involved in cortical development and patterning, including *Foxg1, Pax6*, *Emx1, Emx2, Nr2f1 (Coup-TF1)* and *Sp8* (Fig. 6*B* and *C*). Similarly, genes associated with development of the cortical hem, *Lmx1a* and *Msx1,* were significantly downregulated in *Dmrta2*$^{-/-}$ cultures. Interestingly, *Dmrta2* itself was identified as one of the most significantly upregulated transcripts upon loss of *Dmrta2* (Fig. 6*B* and Fig. S5*C*). The closely-related *Dmrt* family member *Dmrta1* was also upregulated in *Dmrta2*$^{-/-}$ NPCs, while no significant change was found for *Dmrt3*. In the reduced cortex of *Dmrta2* conditional mutants, *Dmrta2* and *Dmrta1* have been also found to be upregulated (14). Together, these observations further support a negative autoregulatory function for *Dmrta2*, as well as regulatory interactions with other *Dmrt* family members.

We are particularly interested in genes and gene-sets that have a functional role in NPC proliferation and/or neuronal differentiation. Our data revealed a significant downregulation of *Hes1* (Fig. 6*C*). Downregulated expression was also identified for other transcription factors known to complex with *Hes1* to repress proneural gene expression and promote NPC proliferation, including *Id1, Id3 and Tcf3* (6, 26, 27). In contrast, we found an upregulation in the expression of *Hes1* target proneural genes *Neurog1*, *Neurog2* and *Ascl1,* together with their downstream target genes *Neurod1, Neurod4* and *Nhlh1 (3, 4)*.

Furthermore, genes known to perform opposing actions to *Hes1* by promoting the expression of proneural genes were upregulated, including *Pax6* and *Btg2* (5, 28). Other upregulated transcription factors with pro-neuronal functions included *Insm1*, *Myt1l* and *Brn2 (29, 30)*. Consistent with these findings, molecular markers for intermediate progenitor (*Eomes*), immature (*Dcx*) and mature (*Mapt*, *Nefh* and *Rbfox3*) neurons were also upregulated in *Dmrta2*$^{-/-}$ cells (Fig. 6*D*).

To provide a broader overview of the cellular functions played by *Dmrta2*-regulated genes/gene-sets, we performed a gene ontology functional enrichment analysis using gene lists meeting the stringent criteria of $p<0.01$ and an absolute fold change value greater than two. This analysis revealed that the 650 upregulated genes meeting these criteria are enriched in transcripts associated with biological processes including neuronal differentiation, neurogenesis and nervous system development in general (Fig. S5*A*). Similarly, enrichments for genes linked to the regulation of cell proliferation, organ morphogenesis and locomotion were identified in 936 transcripts downregulated in *Dmrta2*$^{-/-}$ cortical NPCs (Fig. S5*B*). Together, our global gene expression analysis provides strong independent support that Dmrta2 plays a role in balancing NPC proliferation and neurogenesis.

Dmrta2-controlled neuronal differentiation involves direct regulation of *Hes1*

The significant downregulation of *Hes1* revealed by the RNAseq analysis in addition to its robust induction in response to *Dmrta2* transgene expression in NPCs suggests that Dmrta2 may maintain cortical NPC status via regulating *Hes1* transcription. To determine whether this is mediated by direct binding of Dmrta2, we performed chromatin immunoprecipitation (ChIP) on day 8 *Dmrta2*$^{flox/flox}$ NPCs, with *Dmrta2*$^{-/-}$ NPCs serving as a negative control. Based on the published consensus binding sequence for Dmrta2, we identified three potential binding sites (Bs1-3) at the *Hes1* locus (Fig. 7*A*) (31). Dmrta2-immunoprecipitation of DNA fragments at each of these sites was quantified relative to a non-bound control region (NBCR) by qPCR (Fig. 7*B*). An enrichment in Dmrta2-bound fragments was identified at binding sites Bs1 and Bs2 ($p<0.05$) but not in Bs3 in *Dmrta2*$^{flox/flox}$ cells. In contrast, no enrichment was detected at any of the three potential binding sites in *Dmrta2*$^{-/-}$ negative control cells. Thus, Dmrta2 binds to the *Hes1* gene in NPCs.

To provide evidence for Dmrta2 regulatory activity at Bs1 and Bs2, we performed reporter assays using a *Hes1* promoter-driven luciferase vector (32). A two-fold higher basal *Hes1* promoter activity level was recorded in the isogenic *Dmrta2*$^{flox/flox}$ cultures relative to the *Dmrta2*$^{-/-}$ NPCs on day 8 of differentiation ($p<0.001$) (Fig. 7*C*). An A>C point mutation at position -3 of the binding motif has been shown to significantly impair the ability of Dmrta2 to bind to its target sequence (31). We therefore introduced A>C point mutations at Bs1 and Bs2 by site-directed mutagenesis to yield two mutated reporter constructs, p*Hes1*-luc-Bs1g.2007A>C and p*Hes1*-luc-Bs2g.2365A>C, respectively. The mutation at Bs1, but not Bs2, resulted in a significant reduction of elevated *Hes1* promoter activity levels in *Dmrta2*$^{flox/flox}$ NPCs relative to the parental luciferase construct ($p<0.01$), suggesting reduced binding of Dmrta2 to the mutated Bs1 (Fig. 7*C*). Together these data strongly support the ability of Dmrta2 to bind to and regulate transcriptional activity at Bs1 on the *Hes1* genomic locus.

We next sought to determine the extent to which reduced *Hes1* expression in *Dmrta2*$^{-/-}$ NPCs may contribute to their altered neurogenesis. To this end, *Dmrta2*$^{flox/flox}$ and *Dmrta2*$^{-/-}$ NPCs were transfected with a *Hes1*-expression vector on day 6 of differentiation together with a GFP-coding plasmid to distinguish between *Hes1*-transfected and non-transfected cells (Fig. 7*D*). By quantifying Tubb3 staining 48 hours post-transfection, we identified

significantly increased numbers of neurons in the non-transfected population of *Dmrta2*$^{-/-}$ cells relative to non-transfected isogenic controls ($p<0.01$). As predicted based on known Hes1 function, *Hes1* transgene expression led to a reduction in neuronal production for each cell line. Interestingly, no significant differences between cell lines were identified within the *Hes1* transfected populations. Thus, *Hes1* trangene expression leads to a rescue of the precocious neurogenesis associated with the loss of Dmrta2.

We then asked whether siRNA-mediated knockdown of *Hes1* expression could attenuate the anti-neurogenic effect of *Dmrta2* transgenic expression in cortical NPCs. *Dmrta2*-ESCs were treated with doxycycline and *Hes1*-siRNA or a control non-targeting siRNA from day 5 to 12 of differentiation. *Hes1*-knockdown resulted in a significant reduction of Nestin^{+} NPCs ($p<0.05$) and concurrent increase in the proportion of Tubb3^{+} neuronal cells (Fig. 7*E*). Thus, Hes1 knockdown partially reverses Dmrta2-mediated suppression of neuronal differentiation.

Together, our data identify *Hes1* as a downstream target of Dmrta2 transcriptional regulation and a mechanism through which Dmrta2 safeguards NPCs from premature differentiation.

Discussion

Dmrta2 in NPC cell cycle regulation

Loss-of-function mutations in *Dmrta2* have been linked with microcephaly in zebrafish, mice and humans (7, 10-13). However, the role and mechanism of action of Dmrta2 in the control of NPC maintenance and expansion remains, until now, completely unknown. Recently, conditional *Dmrta2* mutant mice (*Dmrta2*$^{fl/fl}$*;Emx1-cre*) have been created that delete *Dmrta2* in cortical progenitors after cortical hem formation without impacting Wnt signalling. The Dmrta2 cKO embryos also show reduced cortical hemisphere size suggesting a direct role of Dmrta2 in the control of NPC behaviour (14). Cells in a monolayer ESC-neural differentiation system are by and large exposed to the same extracellular environment and don't form 'signalling centres' as those found in the developing brain. Moreover, daily changes of culture media will reduce the impact of any secreted molecules that may elicit a secondary effect. Our pathway analysis of the RNAseq data did not reveal any significant changes in Wnt signalling, therefore, the observed effect of Dmrta2 on cell cycle changes is likely cell autonomous.

In line with the accumulation of *Dmrta2*$^{-/-}$ NPCs in the G0/G1 phase of the cell cycle, our study reported the altered expression of a number of cell cycle regulatory genes, particularly those acting on the G1 to S phase transition (*Cdkn1b*, *Cdkn1c* and *Btg2*). Together, these data suggest a disruption in cell cycle progression and potential lengthening of the G1 phase in *Dmrta2*$^{-/-}$ NPCs. During normal corticogenesis the duration of the G1 phase is linked to neuronal differentiation and is always higher in cells committed to undergo differentiative rather than proliferative divisions (33, 34). Furthermore, experimental lengthening of the G1 phase pharmacologically or by the induction of *Cdkn1b* or *Cdkn1c* expression promotes neuronal differentiation and depletion of the NPC pool resulting in microcephaly (1, 33, 35). The observed increase of *Cdkn1b* and *Cdkn1c* in *Dmrta2*$^{-/-}$ NPCs strongly implicates delayed cell cycle progression of *Dmrta2*$^{-/-}$ NPCs as a cellular mechanism contributing to precocious neurogenesis. However, it is unclear at present whether this is achieved through the direct regulation of cell cycle progression genes by Dmrta2. Although a number of G1-S transition regulatory molecules are known to act as downstream targets for *Hes1* repression, *Cdkn2c* (p18ink4c) has also been identified as a candidate gene for direct *Dmrta2*-mediated regulation in the zebrafish testes (11, 36, 37). Whether or not through a direct effect, our study demonstrates that Dmrta2 is intricately linked with the control of cell cycle progression, a feature conserved across species and tissues.

In addition to their function in the regulation of cell cycle progression, cyclin-dependent kinase inhibitors, including *Cdkn1b*, directly influence and promote NPC differentiation by stabilising protein levels of *Neurog2* via direct binding and the regulation of both interkinetic and radial migration (35, 38, 39). The transcriptome analysis of *Dmrta2*$^{-/-}$ NPCs identified an enrichment of downregulated transcripts associated with gene ontology terms for cell adhesion (GO:0007155) and locomotion (GO:004001). It is therefore possible that defective migration is a cellular phenotype associated with the loss of *Dmrta2* that could potentially lead to increased neuronal differentiation. Similarly, our RNAseq data alludes to a potential switch in the mode of cell division of *Dmrta2*$^{-/-}$ NPCs. The transcription factors *Emx2* and *Pax6* were found to be downregulated and upregulated, respectively, by *Dmrta2*$^{-/-}$ NPCs, as well as in the brains of *Dmrta2*-null mice (12). Further to their roles in telencephalic patterning, Emx2 is known to promote symmetric proliferative division of NPCs and Pax6 asymmetric differentiative division (40, 41). Thus, a switch in the mode of proliferation to neurogenic divisions may be a further cellular feature contributing to increased differentiation in the absence of Dmrta2. This is supported by the strong upregulation of mRNA transcripts for *Btg2* which is exclusively expressed in cortical NPCs committed to undergoing neurogenic but not proliferative divisions (42). Thus, while we provide evidence that *Dmrta2* safeguards NPCs from precocious neurogenesis via regulation of *Hes1*, other targets may also contribute to the fine control of neurogenesis by *Dmrta2*.

Dmrta2 targets and neurogenesis

To date, *Hes1* and *Cdkn2c* are the only two transcriptional targets proposed for *Dmrta2*. Due to high levels of conservation in DNA binding motifs between Dmrt proteins, further insight may be provided by examining DNA binding sites of related Dmrt family members in other tissues (31). Close to 1,400 direct binding sites for Dmrt1 in the mouse testis have been identified using ChIP-chip techniques (43). Many of these genes were also identified as dysregulated by our *Dmrta2*$^{-/-}$ NPC transcriptome analysis, including: *Cdkn2c*, *Igf2r*, *Meis1*, *Hox* family members and other *Dmrt* genes. Although *Dmrt1* is not expressed by cortical NPCs, our data suggests significant overlaps in the regulatory targets of different *Dmrt* proteins. This is of particular interest due to the similar expression patterns of *Dmrt*3, *Dmrta1* and *Dmrta2* in the dorsal telencephalon suggesting a potential for functional redundancy (13, 24). A similar but less severe phenotype to that seen in *Dmrta2* null mutants has been observed in mice with a *Dmrt3* null mutation, further supporting the idea that the two factors have overlapping function in cortical development (12-14). In contrast, *Dmrta1*-null mice produce viable offspring with no overt anatomical defects in the brain (13, 44). This implies a hierarchical structure of importance of the *Dmrt* proteins to cortical development. Similar to our transgenic *Dmrta2* findings, forced expression of *Dmrt3* or *Dmrta1* in the rodent telencephalon is linked to the regulation of *Neurog2* expression (24). Further studies may reveal to what extent this functional overlap exists between Dmrt family members in the dorsal telencephalon.

The functions of the Notch target gene *Hes1* in maintaining NPC self-renewal have been well characterised (6). Notch ligands produced by newborn neurons activate notch signalling in neighbouring cells which in turn induces expression of Hes1 to repress the transcription of proneural factors and cell cycle progression regulators, thereby inhibiting neuronal differentiation (6, 36, 37). This lateral inhibition of spontaneous neuronal differentiation by neighbouring cells favours NPC proliferation and self-renewal. However, *Hes1* expression is dynamically regulated by a number of mechanisms including: a strong negative autoregulatory function, which is in turn inhibited by interactions with Id proteins (45, 46); the activity of other transcription factors, such as Lhx2 (47); and the activation of signalling pathways by growth factors and mitogens including Fgf2 and Notch (6, 48). Under healthy conditions, these homeostatic mechanisms help maintain a NPC pool through development

by regulating the expression of *Hes1* and, therefore, the balance between progenitor cell self-renewal and differentiation. This study identifies *Dmrta2* as a novel factor contributing to the dynamic regulation of *Hes1* expression in cortical NPCs. By promoting *Hes1*, and thereby suppressing downstream proneural gene expression, *Dmrta2* helps contribute to the maintenance of NPC self-renewal (Fig. 8*A*). In the absence of *Dmrta2*, *Hes1* levels are reduced, leading to the upregulation of proneural genes and increased neuronal differentiation (Fig. 8*B*).

In summary, we have identified *Dmrta2* as a modulator controlling neuronal differentiation of cortical NPCs and provided evidence that *Dmrta2* exerts this function, at least in part, by direct transcriptional regulation of neurogenesis inhibitor *Hes1*. Thus, this work points to another layer of control mechanisms coordinating NPC maintenance and neurogenesis, and begin to elucidate how *Dmrta2* loss-of-function mutations may lead to microcephaly.

Materials and Methods

Cell culture

Six mouse ESC lines were used: a *Dmrta2*$^{flox/flox}$ control line and two *Dmrta2*$^{-/-}$ lines derived from the control line line (SI Materials and Methods), two independent doxycycline inducible *Dmrta2* overexpression ESC lines and their parental lines harbouring rtTA as reported previously (9). All ESCs were maintained under standard conditions as previously described (17). For monolayer based cortical differentiation, ESCs were seeded at 10 000 cells/cm^2 in gelatin-coated 6 well plates and cultured in N2B27 medium. Differentiation medium was supplemented with 100 nM LDN193189, 10 µM SB431542 from days 0 to 4, 1 µM XAV939 from day 0 to 6 (all Tocris) and 1 µM cyclopamine between days 2 and 10 (Sigma-Aldrich). On day 5 or 6 of differentiation, neural progenitor cells were dissociated using Trypsin/EDTA and replated onto poly-D-lysine/laminin coated surface at a density of 50,000 cells/cm^2 for neuronal differentiation and maturation.

Transient transfections were performed using lipofectamine 3000 reagent (Thermofisher Scientific). The following vectors were used: p*Hes1*(2.5k)-luc (Addgene) (32); pGL4.73[hR*luc*/SV40] (Promega); pCAG-*Hes1*-IP and pmaxGFP (Lonza). Accell *Hes1* and non-targeting control siRNA (GE Dharmacon) were used at a concentration of 1 µM.

Mouse Lines

Emx1-cre and *Dmrta2*$^{fl/fl}$ mouse lines were generated and maintained as previously described (14).

Quantitative RT-PCR (qPCR)

Total RNA was extracted using Tri reagent treated with TURBO DNase. cDNA was generated using qScript cDNA synthesis kit. qPCR was performed with Mesa Green qPCR master mix with specific primers listed in Table S1 and dissociation curves were recorded to check for amplification specificity. Cq values were normalised to a minimum of two housekeeping reference genes and changes in expression calculated using the $2^{-\Delta\Delta CT}$ method (49). Three independent experiments were performed (n=3) and each sample measured in duplicate on a CFX Connect Real Time PCR machine.

Immunocytochemistry and EdU-labelling

Cultures were fixed with 4% (w/v) paraformaldehyde and permeabilised with 0.1% (v/v) Triton X-100. Following blocking with 2% (w/v) bovine serum albumin and 5% (v/v) donkey serum, cells were incubated with primary antibodies overnight at 4°C before incubated with complementary Alexa Fluor-conjugated antibodies and counterstained with DAPI. All antibodies used are listed in SI Materials and Methods. To quantify proliferation, differentiating cultures were incubated with 5 µM EdU for 30 minutes before fixation. EdU

detection was then carried out using the Click-iT EdU Alexa Fluor 488 imaging kit (Life Technologies, UK). Images were subsequently acquired using a DMI600b inverted microscope (Leica Microsystems). Manual cell counts were performed on a minimum of 10 randomly placed fields of view per stain and the mean of three separate differentiations calculated (n=3).

Embryo sections (6-8 µm) fixed overnight in 4% paraformaldehyde/PBS, dehydrated and paraffin-embedded were processed as described previously (14). For quantification of cells expressing Tubb3, cells of the entire dorsal telencephalon at the medial level were counted (at least 2 embryos of each genotype were analysed with a quantification of 3 to 6 sections/embryo).

Cell cycle analysis by flow cytometry

NPCs were dissociated with EDTA, washed in PBS and fixed with ice-cold 70% ethanol. After washing with 1% BSA, cell samples were incubated with mouse anti-Nestin (BD Biosciences, 611659, 1 µg/ml) or mouse IgG isotype (Sigma-Aldrich, I5381, µg/ml) antibodies overnight at 4°C. Following incubation with donkey anti-mouse Alexa-Flour 647 secondary antibody (Thermofisher Scientific, A-31571, 1:1000), DNA content was labelled by incubating cells with 1 µg/ml DAPI. Stained cells were analysed on an Amnis Flowsight (Merck Millipore) under excitation from 405 nm and 642 nm lasers. IgG isotype control samples were used to set gating parameters for nestin^{+} neural progenitor cells and DAPI staining to identify cells at different stages of the cell cycle. Samples from three individual differentiation experiments were analysed for each time point (n=3).

RNAseq

RNA was extracted and purified using the PureLink RNA Mini Kit (Thermofisher Scientific). TruSeq Stranded mRNA kit (Illumina) was used to prepare libraries from 1 µg RNA from 3 independent differentiations (n=3). 75bp paired-end sequencing was performed on a HiSeq 4000 (Illumina, USA) yielding 30 – 45 million reads per sample. Reads were mapped to the mouse genome (mm10, GRCm38) using Burrows-Wheeler Aligner algorithms (50) and individual gene read counts calculated using featureCounts (51). DeSeq2 was used to calculate differential gene expression (52). Gene Ontology functional enrichment for biological processes was performed using DAVID (v6.8) with mus musculus genome set as background (53). Calculated p values were adjusted for multiple testing using the Benjamini-Hochberg correction. Raw sequence data files are publically available from the NCBI Gene Expression Omnibus (GEO accession: GSE90827).

Luciferase reporter assays

Point mutations were introduced into the p*Hes1*(2.5k)-luc firefly luciferase vector using a Quikchange II XL Site-Directed Mutagenesis kit (Agilent Technologies) and the mutagenic primers (5'→3'): CAAGGTAAAGAGGATGTGTTCCTCTAATGTCTTCCGGAATT and AATTCCGGAAGACATTAGAGGAACACATCCTCTTTACCTTG for Bs1; and GAAAGTTCCTGTGGGAAAGAAAGTTTGGGAAGTTTCAC and CAAACTTTCTTTCCCACAGGAACTTTCAGCCAATGG for Bs2. Generation of mutagenized plasmids were confirmed by sanger sequencing.

For luciferase reporter assays, cells were cultured in 24-well plates and co-transfected with 290 ng/well firefly luciferase (p*Hes1*(2.5k)-luc and it's derivatives). 10 ng/well of renilla luciferase vector (pGL4.73) was used as an internal control to normalise for transfection efficiency and 50 ng of notch intracellular domain (NICD (pCAG-NotchIC-IP) served as a positive control. Cells were harvested 24 hours post-transfection and processed using the Dual-Glo Luciferase Assay System (Promega). Luciferase activity was measured with

GloMax 96 Microplate Luminometer (Promega). Triplicate readings were taken for each sample and all experiments repeated with three biological replicates (n=3).

Chromatin immunoprecipitation (ChIP)
Approximately 10^7 cells on day 8 of differentiation were used per immunoprecipitation. Protein and DNA were cross-linked with 1% formaldehyde before cell lysis. The extracted chromatin was subsequently sonicated at high power for 20 cycles of 30 seconds on/30 seconds off with a Bioruptor (Diagenode). Immunoprecipitation was performed by incubating chromatin with custom rabbit anti-Dmrta2 or rabbit IgG isotype control antibodies and Salmon Sperm DNA/Protein A Agarose Beads (Merck Millipore). Following denaturation of crosslinks, Dmrta2-bound DNA fragments were purified using the Wizard SV Gel and PCR Clean-Up System (Promega). Immunoprecipitated DNA was subsequently amplified in qPCR reactions using the primers specified in Supplementary table 1. Two immunoprecipitations, each from a separate differentiation experiment, were performed (n = 2).

Statistical Analysis
Statistical analyses were performed using IBM SPSS 20 software. Where specified, two way ANOVA tests were performed using Dmrta2 genotype status and day of differentiation as independent variables. Simple effects analysis by post-hoc Sidak's test was used to correct for separate orthogonal comparisons between groups at each time point and to identify statistical significance. For luciferase assays and siRNA knockdown experiments one way ANOVA with Tukey-HSD post-hoc tests were performed. One tailed and two-tailed Student's t-tests were used to analyse ChIP-qPCR and *Hes1*-transfection rescue experiments, respectively.

Acknowledgements
We thank Drs. Sally Lowell for pCAG-NotchIC and Ryoichiro Kageyama for Hes1-luciferase vectors. Thanks also to Mr. Dani Cabezas de la Fuente and Dr. Andrew Roberts for invaluable assistance with bioinformatics analysis. RNA sequencing was performed at the Oxford Genomics Centre. This work is funded by UK Medical Research Council and Cardiff Neuroscience and Mental Health Research Institute.

Footnotes
‡**Corresponding author:** Meng Li, Email: LiM26@cardiff.ac.uk Tel: +44-29-20688345; ebellefr@ulb.ac.be Tel: +32 26509732

Author contributions: F.I.Y., N.G. and M.L. designed research, X.N. generated all the Dmrta2 cell lines and mutagenized luciferase plasmids; F.I.Y. performed research on Dmrta2 knockout cells. N.G. carried out studies with the Dmrta2 overexpression cells. M.K. and E.J.B. designed and performed research with conditional *Dmrta2* mutant mice. F.I.Y., M.K., N.G. and M. L. analysed the data; F.I.Y. and M. L. wrote the paper with critical comments from X.N., M.K and E.J.B.

The authors declare no conflict of interest.

References

1. Caviness Jr VS*, et al.* (2003) Cell output, cell cycle duration and neuronal specification: A model of integrated mechanisms of the neocortical proliferative process. *Cerebral Cortex* 13(6):592-598.
2. Miyata T, Kawaguchi D, Kawaguchi A, & Gotoh Y (2010) Mechanisms that regulate the number of neurons during mouse neocortical development. *Current Opinion in Neurobiology* 20(1):22-28.
3. Seo S, Lim JW, Yellajoshyula D, Chang LW, & Kroll KL (2007) Neurogenin and NeuroD direct transcriptional targets and their regulatory enhancers. *EMBO Journal* 26(24):5093-5108.
4. Gohlke JM*, et al.* (2008) Characterization of the proneural gene regulatory network during mouse telencephalon development. *BMC Biology* 6.
5. Sansom SN*, et al.* (2009) The level of the transcription factor Pax6 is essential for controlling the balance between neural stem cell self-renewal and neurogenesis. *PLoS Genetics* 5(6).
6. Imayoshi I & Kageyama R (2014) bHLH factors in self-renewal, multipotency, and fate choice of neural progenitor cells. *Neuron* 82(1):9-23.
7. Urquhart JE*, et al.* (2016) DMRTA2 (DMRT5) is mutated in a novel cortical brain malformation. *Clinical Genetics* 89(6):724-727.
8. Bellefroid EJ*, et al.* (2013) Expanding roles for the evolutionarily conserved Dmrt sex transcriptional regulators during embryogenesis. *Cellular and Molecular Life Sciences* 70(20):3829-3845.
9. Gennet N*, et al.* (2011) Doublesex and mab-3-related transcription factor 5 promotes midbrain dopaminergic identity in pluripotent stem cells by enforcing a ventral-medial progenitor fate. *Proceedings of the National Academy of Sciences of the United States of America* 108(22):9131-9136.
10. Yoshizawa A*, et al.* (2011) Zebrafish Dmrta2 regulates neurogenesis in the telencephalon. *Genes to Cells* 16(11):1097-1109.
11. Xu S, Xia W, Zohar Y, & Gui JF (2013) Zebrafish dmrta2 regulates the expression of cdkn2c in spermatogenesis in the adult testis. *Biology of Reproduction* 88(1).
12. Saulnier A*, et al.* (2013) The doublesex homolog Dmrt5 is required for the development of the caudomedial cerebral cortex in mammals. *Cerebral Cortex* 23(11):2552-2567.
13. Konno D*, et al.* (2012) The Mammalian DM Domain Transcription Factor Dmrta2 Is Required for Early Embryonic Development of the Cerebral Cortex. *PLoS ONE* 7(10).
14. De Clercq S*, et al.* (2016) DMRT5 Together with DMRT3 Directly Controls Hippocampus Development and Neocortical Area Map Formation. *Cerebral Cortex*.
15. Caronia-Brown G, Yoshida M, Gulden F, Assimacopoulos S, & Grove EA (2014) The cortical hem regulates the size and patterning of neocortex. *Development (Cambridge)* 141(14):2855-2865.
16. Hirabayashi Y*, et al.* (2004) The Wnt/β-catenin pathway directs neuronal differentation of cortical neural precursor cells. *Development* 131(12):2791-2801.
17. Ying QL, Stavridis M, Griffiths D, Li M, & Smith A (2003) Conversion of embryonic stem cells into neuroectodermal precursors in adherent monoculture. *Nature Biotechnology* 21(2):183-186.
18. Gaspard N*, et al.* (2008) An intrinsic mechanism of corticogenesis from embryonic stem cells. *Nature* 455(7211):351-357.
19. Cambray S*, et al.* (2012) Activin induces cortical interneuron identity and differentiation in embryonic stem cell-derived telencephalic neural precursors. *Nature Communications* 3.
20. Chambers SM*, et al.* (2009) Highly efficient neural conversion of human ES and iPS cells by dual inhibition of SMAD signaling. *Nature Biotechnology* 27(3):275-280.
21. Watanabe K*, et al.* (2005) Directed differentiation of telencephalic precursors from embryonic stem cells. *Nature Neuroscience* 8(3):288-296.

22. Bertacchi M, Pandolfini L, D'Onofrio M, Brandi R, & Cremisi F (2015) The double inhibition of endogenously produced bmp and wnt factors synergistically triggers dorsal telencephalic differentiation of mouse es cells. *Developmental Neurobiology* 75(1):66-79.
23. Jaeger I*, et al.* (2011) Temporally controlled modulation of FGF/ERK signaling directs midbrain dopaminergic neural progenitor fate in mouse and human pluripotent stem cells. *Development* 138(20):4363-4374.
24. Kikkawa T*, et al.* (2013) Dmrta1 regulates proneural gene expression downstream of Pax6 in the mammalian telencephalon. *Genes to Cells* 18(8):636-649.
25. Barbelanne M & Tsang WY (2014) Molecular and cellular basis of autosomal recessive primary microcephaly. *BioMed Research International* 2014.
26. Lyden D*, et al.* (1999) Id1 and Id3 are required for neurogenesis, angiogenesis and vascularization of tumour xenografts. *Nature* 401(6754):670-677.
27. Nakashima K*, et al.* (2001) BMP2-mediated alteration in the developmental pathway of fetal mouse brain cells from neurogenesis to astrocytogenesis. *Proceedings of the National Academy of Sciences of the United States of America* 98(10):5868-5873.
28. Canzoniere D*, et al.* (2004) Dual Control of Neurogenesis by PC3 through Cell Cycle Inhibition and Induction of Math1. *Journal of Neuroscience* 24(13):3355-3369.
29. Farkas LM*, et al.* (2008) Insulinoma-Associated 1 Has a Panneurogenic Role and Promotes the Generation and Expansion of Basal Progenitors in the Developing Mouse Neocortex. *Neuron* 60(1):40-55.
30. Vierbuchen T*, et al.* (2010) Direct conversion of fibroblasts to functional neurons by defined factors. *Nature* 463(7284):1035-1041.
31. Murphy MW, Zarkower D, & Bardwell VJ (2007) Vertebrate DM domain proteins bind similar DNA sequences and can heterodimerize on DNA. *BMC Molecular Biology* 8.
32. Takebayashi K*, et al.* (1994) Structure, chromosomal locus, and promoter analysis of the gene encoding the mouse helix-loop-helix factor HES-1. Negative autoregulation through the multiple N box elements. *Journal of Biological Chemistry* 269(7):5150-5156.
33. Calegari F, Haubensak W, Haffher C, & Huttner WB (2005) Selective lengthening of the cell cycle in the neurogenic subpopulation of neural progenitor cells during mouse brain development. *Journal of Neuroscience* 25(28):6533-6538.
34. Dehay C & Kennedy H (2007) Cell-cycle control and cortical development. *Nature Reviews Neuroscience* 8(6):438-450.
35. Tury A, Mairet-Coello G, & Dicicco-Bloom E (2011) The cyclin-dependent kinase inhibitor p57Kip2 regulates cell cycle exit, differentiation, and migration of embryonic cerebral cortical precursors. *Cerebral Cortex* 21(8):1840-1856.
36. Castella P, Sawai S, Nakao K, Wagner JA, & Caudy M (2000) Hes-1 repression of differentiation and proliferation in PC12 cells: Role for the helix 3-helix 4 domain in transcription repression. *Molecular and Cellular Biology* 20(16):6170-6183.
37. Murata K*, et al.* (2005) Hes1 directly controls cell proliferation through the transcriptional repression of p27 Kip1. *Molecular and Cellular Biology* 25(10):4262-4271.
38. Nguyen L*, et al.* (2006) p27kip1 independently promotes neuronal differentiation and migration in the cerebral cortex. *Genes and Development* 20(11):1511-1524.
39. Kawauchi T, Shikanai M, & Kosodo Y (2013) Extra-cell cycle regulatory functions of cyclin-dependent kinases (CDK) and CDK inhibitor proteins contribute to brain development and neurological disorders. *Genes to Cells* 18(3):176-194.
40. Heins N*, et al.* (2001) Emx2 promotes symmetric cell divisions and a multipotential fate in precursors from the cerebral cortex. *Molecular and Cellular Neuroscience* 18(5):485-502.
41. Heins N*, et al.* (2002) Glial cells generate neurons: The role of the transcription factor Pax6. *Nature Neuroscience* 5(4):308-315.
42. Iacopetti P*, et al.* (1999) Expression of the antiproliferative gene TIS21 at the onset of neurogenesis identifies single neuroepithelial cells that switch from proliferative to

neuron-generating division. *Proceedings of the National Academy of Sciences of the United States of America* 96(8):4639-4644.
43. Murphy MW*, et al.* (2010) Genome-wide analysis of DNA binding and transcriptional regulation by the mammalian Doublesex homolog DMRT1 in the juvenile testis. *Proceedings of the National Academy of Sciences of the United States of America* 107(30):13360-13365.
44. Balciuniene J, Bardwell VJ, & Zarkower D (2006) Mice mutant in the DM domain gene Dmrt4 are viable and fertile but have polyovular follicles. *Molecular and Cellular Biology* 26(23):8984-8991.
45. Hirata H*, et al.* (2002) Oscillatory expression of the BHLH factor Hes1 regulated by a negative feedback loop. *Science* 298(5594):840-843.
46. Bai G*, et al.* (2007) Id Sustains Hes1 Expression to Inhibit Precocious Neurogenesis by Releasing Negative Autoregulation of Hes1. *Developmental Cell* 13(2):283-297.
47. Chou SJ & O'Leary DDM (2013) Role for Lhx2 in corticogenesis through regulation of progenitor differentiation. *Molecular and Cellular Neuroscience* 56:1-9.
48. Sato T*, et al.* (2010) FRS2α regulates Erk levels to control a self-renewal target Hes1 and proliferation of FGF-responsive neural stem/progenitor cells. *Stem cells (Dayton, Ohio)* 28(9):1661-1673.
49. Livak KJ & Schmittgen TD (2001) Analysis of relative gene expression data using real-time quantitative PCR and the 2-ΔΔCT method. *Methods* 25(4):402-408.
50. Li H & Durbin R (2009) Fast and accurate short read alignment with Burrows-Wheeler transform. *Bioinformatics* 25(14):1754-1760.
51. Liao Y, Smyth GK, & Shi W (2014) FeatureCounts: An efficient general purpose program for assigning sequence reads to genomic features. *Bioinformatics* 30(7):923-930.
52. Love MI, Huber W, & Anders S (2014) Moderated estimation of fold change and dispersion for RNA-seq data with DESeq2. *Genome Biology* 15(12).
53. Huang DW, Sherman BT, & Lempicki RA (2009) Systematic and integrative analysis of large gene lists using DAVID bioinformatics resources. *Nature Protocols* 4(1):44-57.

Figure legends

Fig. 1. *Dmrta2* expression in ESC-derived cortical NPCs. (*A*) Schematic representation of ESC cortical differentiation protocol. (*B*) Dmrta2 immunostaining on day 6 of differentiation showing co-labelling with other cortical markers. (*C*) Co-localised immunostaining of Dmrta2 and Pax6 in neural rosettes on day 8 of differentiation, with $Eomes^+$ basal progenitor extending distally (*D*) Quantification of the proportion of $Dmrta2^+$ cells between days 4 and 10 of differentiation. Data are presented as mean + s.e.m. of three independent experiments. (*E*) Immunocytochemistry for deep (Bcl11b (Ctip2) and Tbr1) and superficial (Satb2) layer cortical neuronal markers at day 15. (*F*) High magnification images of vGlut1 and Bcl11b staining in dorsal telencephalic neurons. Scale bars: 100 μm.

Fig. 2. Enforced expression of Dmrta2 in NPCs suppresses neuronal differentiation. (*A*) Experimental scheme. Monolayer cultures of *Dmrta2*-ESCs were exposed to doxycycline or vehicle control from day 5 to 12. Cultures were harvested every day from day 6 till 12 and samples processed for qPCR. (*B*) qPCR analysis of the genes indicated from day 6-12. Levels of mRNA expression were normalised to day 5. Error bars indicate means ± s.e.m. of three biological replicates. (*C*) phase contrast view of day 10 cultures treated with doxycycline (bottom) or vehicle (top) from day 5. (*D*) sister cultures as C double stained with antibodies against Nestin (green) and Tubb3 (red). (*E*) day 10 cultures as C double stained for Tubb3 (green) and Dmrta2 (red). Scale bar: 100 μm.

Fig. 3. Loss of *Dmrta2* in cortical NPCs accelerate neurogenesis *in vitro*. (*A*) Day 4 and day 6 cultures were immunostained for Nestin, revealing comparable generation of NPCs in the control and *Dmrta2*$^{-/-}$ cultures. (*B*) qPCR analysis of neuronal differentiation markers. Data are representative of 3 independent differentiation experiments. (*C*) Immunostaining and quantification of cells expressing an immature neuronal marker, Tubb3. Two way ANOVA identified a significant increase in the overall production of Tubb3^{+} neurons by Dmrta2$^{-/-}$ NPCs ($F[1,16]=8.005$, $p=0.012$). (*D*) Immunostaining and quantification of cells expressing mature neuronal marker NeuN. Two way ANOVA revealed a significant increase in the overall maturation of neurons derived from Dmrta2$^{-/-}$ NPCs ($F[1,16]=11.991$, $p=0.003$). Scale bars: 100 μm

Fig. 4. Loss of *Dmrta2* in cortical NPCs accelerate neurogenesis *in vivo*. Immunostaining of Tubb3 and Eomes, left and right panel respectively, on coronal brain sections of E11 embryos. Note the increase of Tubb3^{+} and Tbr2^{+} cells (arrows in right panels) in the *Dmrta2*$^{fl/fl}$*;Emx1-Cre* mutants compared to the controls. The graph is a representation of the number of Tubb3^{+} cells in *Dmrta2*$^{fl/fl}$*;Emx1-Cre* and control embryos. Data are presented as mean ± s.e.m. of three independent experiments; *$p<0.05$, two-tailed Student's t-test. Scale bar: 100 μm.

Fig. 5. Disruption of cell cycle progression in *Dmrta2*$^{-/-}$ NPCs. (*A*) Cell cycle analysis of *Dmrta2*$^{flox/flox}$ and *Dmrta2*$^{-/-}$ NPCs by flow cytometry. NPCs were firstly immunostained with antibodies against Nestin (top), and DNA content measured by DAPI-labelling (bottom). (*B*) Quantification of cell distribution in G0/1, S and G2/M phases of the cell cycle. Data are presented as mean ± s.e.m. of three independent experiments; *$p<0.05$, **$p<0.01$; two-way ANOVA ($F[1,12]=7.109$, $p=0.021$) followed by Sidak's post hoc test. (*C*) Quantification of EdU uptake, and the number of cells expressing cdkn1b (p27kip1) and cdkn1c (p57kip2). Two way ANOVA identified overall reduced proliferation in *Dmrta2*$^{-/-}$ NPCs, as indicated by EdU uptake ($F[1,12]=11.336$, $p=0.006$), and an increase in the proportion of cells staining positive for Cdkn1b ($F[1,12]=20.804$, $p<0.001$) and Cdk1nc ($F[1,12]=10.477$, $p=0.007$). Data are presented as mean ± s.e.m. of three independent experiments. Scale bar: 100 μm.

Fig. 6 Genome wide transcriptome analysis supports a role for Dmrta2 in neurogenesis. (*A*) Heatmap depicting 7343 differentially expressed mRNA transcripts ($p<0.05$) identified by RNAseq. (B-D) Examples of differentially expressed genes associated with telencephalic patterning and development (*B*), transcription factors known to regulate neuronal differentiation (*C*), and markers of different stages of neuronal maturation (*D*).

Fig. 7. *Hes1* is a direct target for Dmrta2 transcriptional regulation in NPCs. (*A*) Schematic representation of the *Hes1* genomic locus showing the relative positions of predicted Dmrta2 binding sites (Bs1 – Bs3) and non-binding control region (NCBR), and the primer pairs used to amplify each region following ChIP. (*B*) ChIP-qPCR for each of the regions depicted in (*B*) using chromatin prepared from *Dmrta2*$^{flox/flox}$ and *Dmrta2*$^{-/-}$ NPCs on day 8 of differentiation. Data are presented as mean fold enrichment relative to the NBCR ± s.e.m. of three immunoprecipitations, each prepared from an independent differentiation experiment; *$p<0.05$; one-tailed Student's t-test. (*C*) Reporter assay performed in *Dmrta2*$^{flox/flox}$ and *Dmrta2*$^{-/-}$ NPCs on day 8 of differentiation using wildtype or mutant *Hes1* promoter-luciferase vectors carrying a point mutation at Bs1 or Bs2, respectively. Data are presented as mean ± s.e.m. of three independent transfections with reporter plasmids; **$p<0.01$; one way ANOVA with Tukey-HSD post-hoc test. (*D*) *Dmrta2*$^{flox/flox}$ and *Dmrta2*$^{-/-}$ NPCs were co-transfected with GFP- and *Hes1*-expression vectors on day 6 of differentiation. Cultures were immunostained for Tubb3 48 hours later. Successfully transfected cells overexpressing *Hes1* were identified based on GFP-expression. Data are

presented as mean ± s.e.m. of three transfections, each from an independent differentiation experiment; *p<0.05; two-tailed Student's t-test. (*E)* Monolayer cultures of *Dmrta2*-ESCs were exposed to doxycycline with or without non-targeting control or Hes1 siRNA from day 5. The proportion of Nestin^{+} NPCs and Tubb3^{+} neurons was quantified at day 12. Data are presented as mean ± s.e.m of >20 individual fields of view; **p<0.05; one way ANOVA with Tukey-HSD post-hoc test.

Fig. 8. Dmrta2 modulates neurogenesis through regulation of *Hes1*. Schematic model depicting the function of *Dmrta2* in the modulation of NPC maintenance and neuronal differentiation. (*A*) High *Dmrta2* expression in cortical NPCs ensures high expression of *Hes1* and low levels of proneural genes, thus promoting NPC maintenance and cortical expansion. (*B*) Upon differentiation, *Dmrta2* expression declines resulting in reduced levels of *Hes1* and higher expression of proneural gene, thus enhancing the differentiation of NPCs into post-mitotic neurons.

Fig. 1

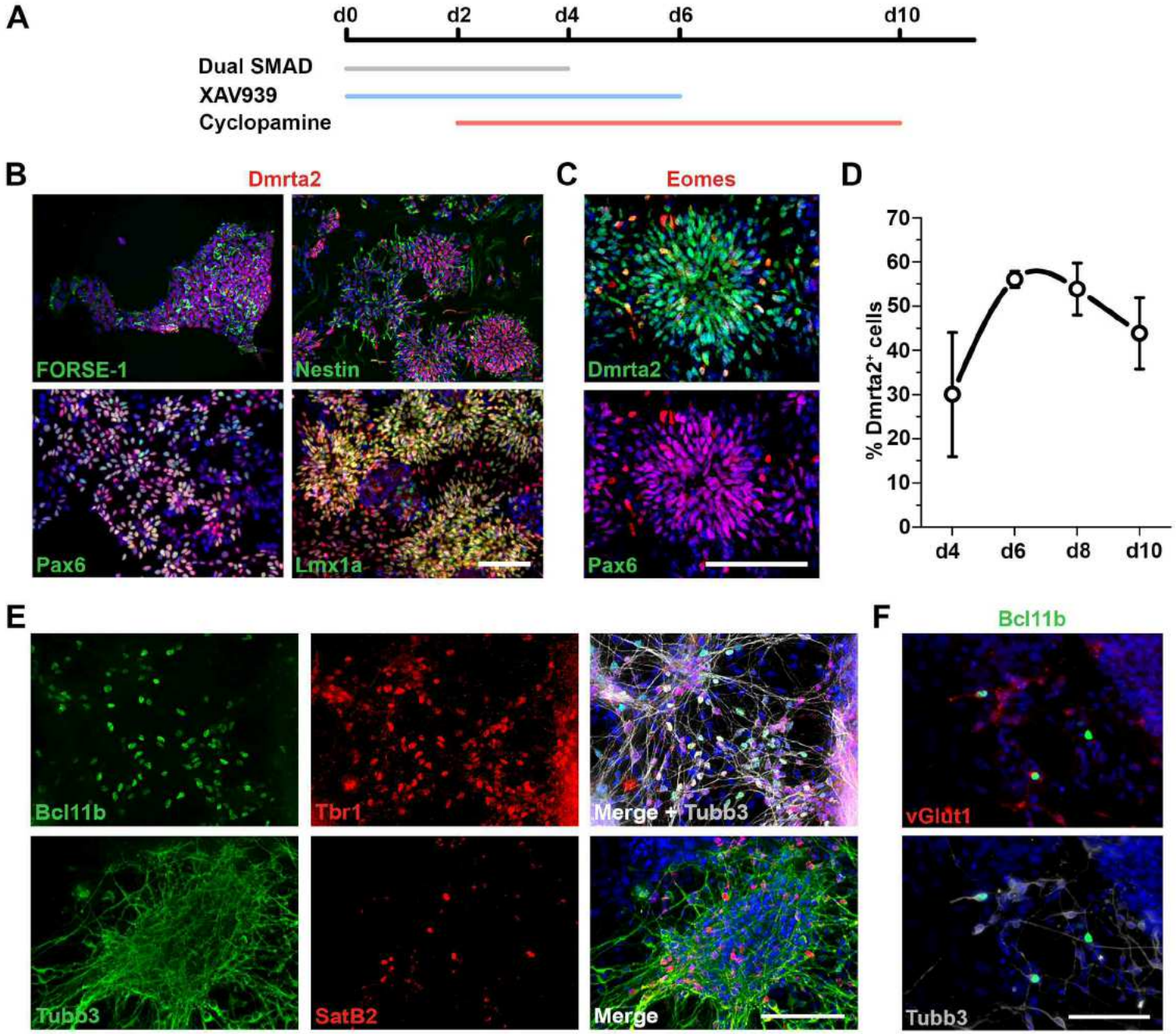
A
d0
d2
d4
d6
d10
Dual SMAD
XAV939
Cyclopamine
B
Dmrta2
FORSE-1
Nestin
Pax6
Lmx1a
C
Eomes
Dmrta2
Pax6
D
% Dmrta2+ cells
70
60
50
40
30
20
10
0
d4
d6
d8
d10
E
Bcl11b
Tbr1
Merge + Tubb3
Tubb3
SatB2
Merge
F
Bcl11b
vGlut1
Tubb3

Fig. 2

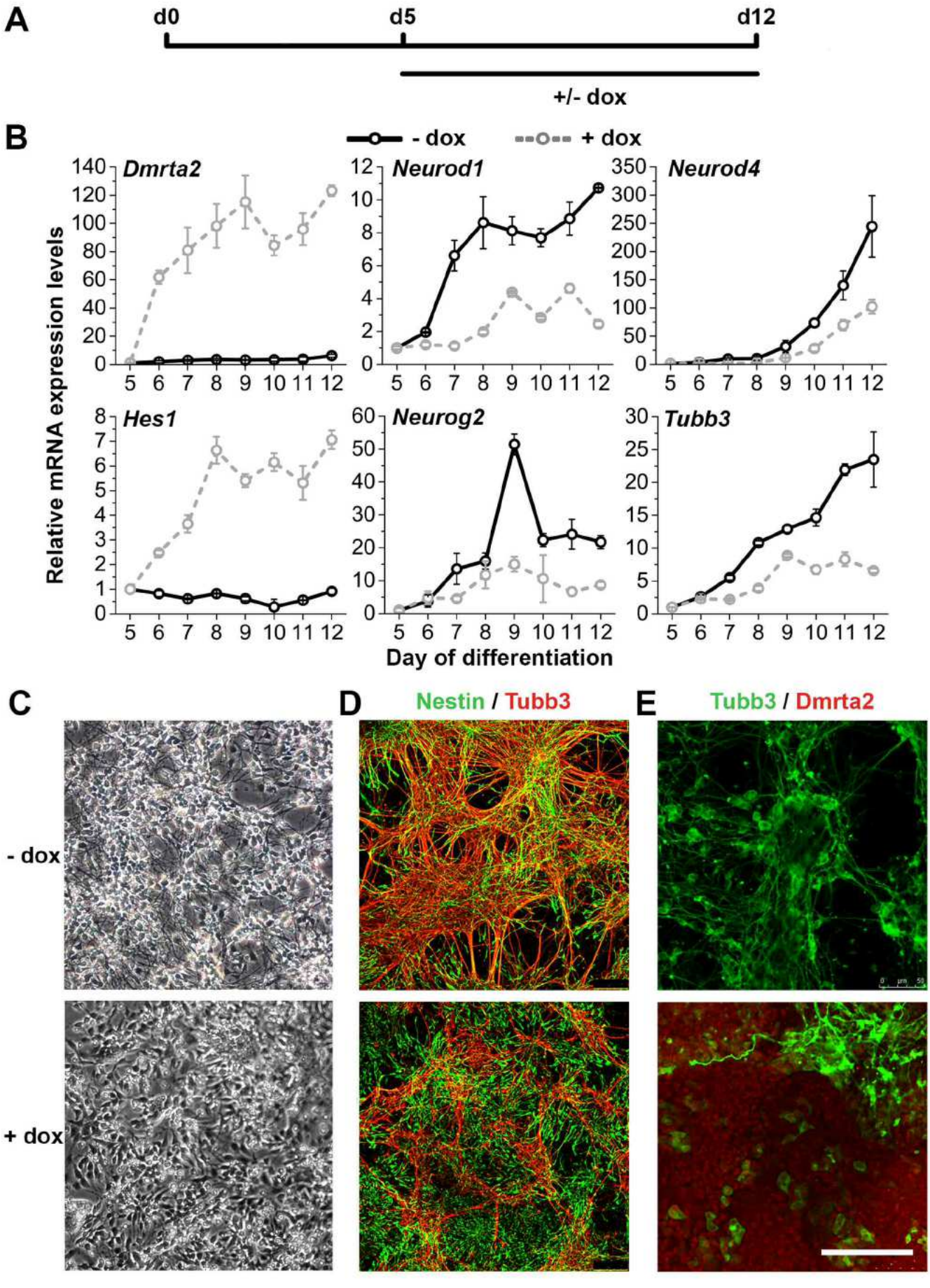
A
d0
d5
d12
+/- dox
B
- dox
+ dox
Dmrta2
Neurod1
Neurod4
Hes1
Neurog2
Tubb3
Relative mRNA expression levels
Day of differentiation
C
D
Nestin / Tubb3
E
Tubb3 / Dmrta2
- dox
+ dox

Fig. 3

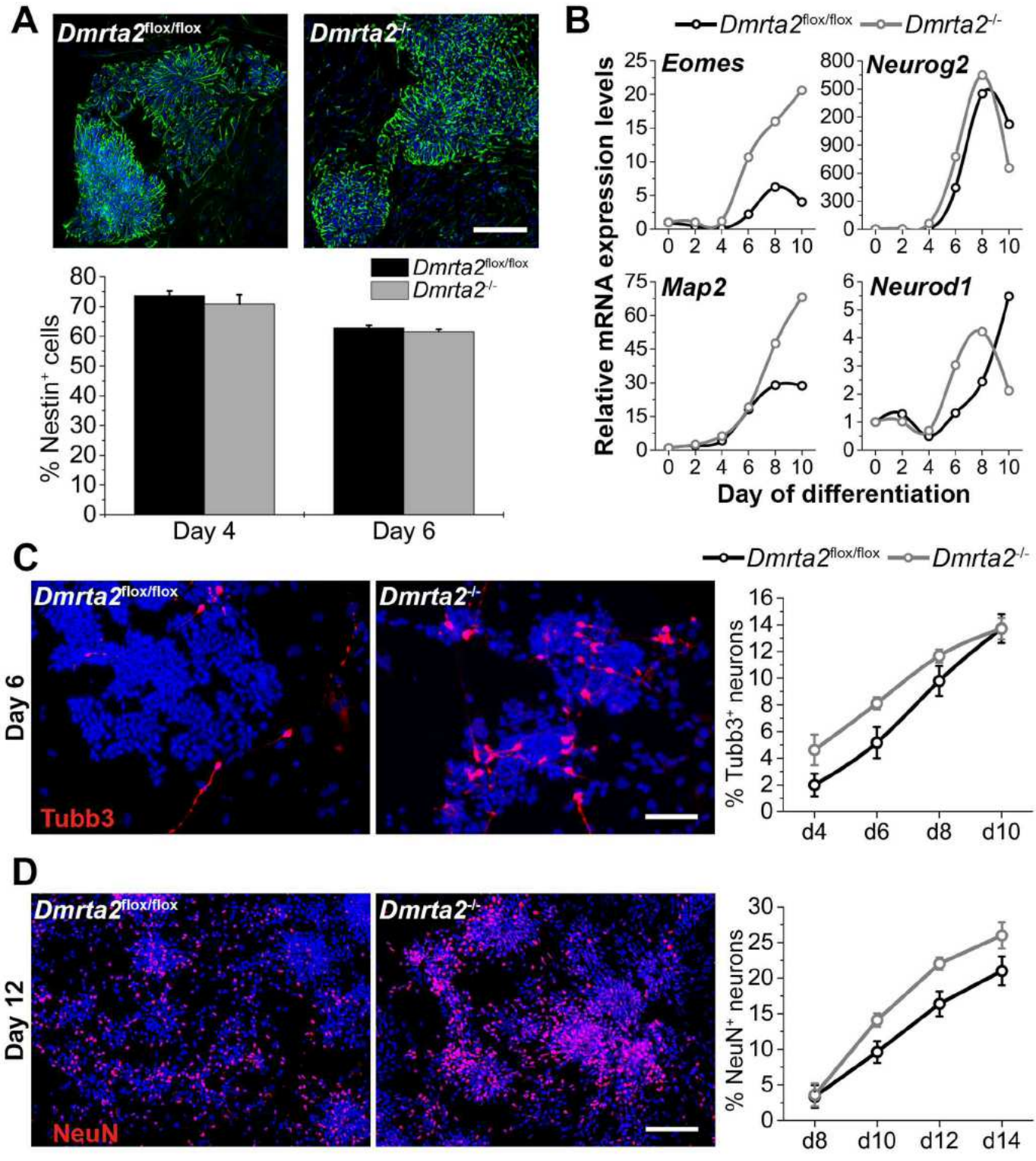
A
Dmrta2flox/flox
Dmrta2-/-
% Nestin+ cells
Day 4
Day 6
B
Dmrta2flox/flox
Dmrta2-/-
Eomes
Neurog2
Map2
Neurod1
Relative mRNA expression levels
Day of differentiation
C
Dmrta2flox/flox
Dmrta2-/-
Day 6
Tubb3
% Tubb3+ neurons
d4
d6
d8
d10
D
Dmrta2flox/flox
Dmrta2-/-
Day 12
NeuN
% NeuN+ neurons
d8
d10
d12
d14

Fig. 4

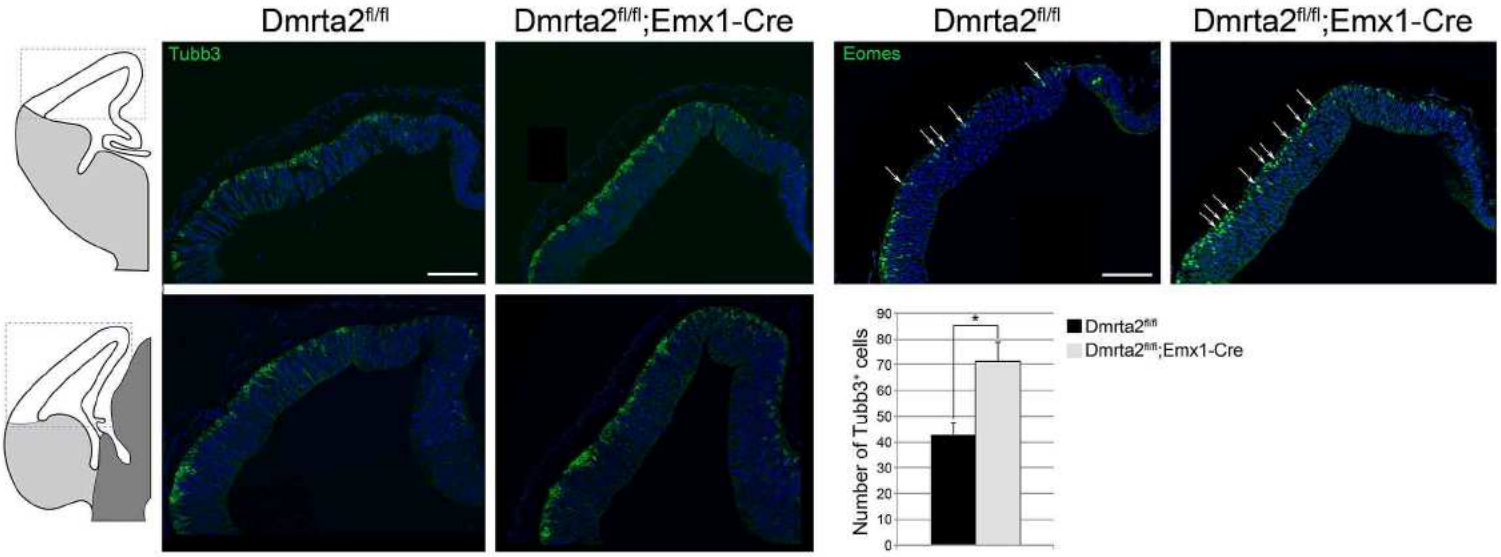
Dmrta2fl/fl
Dmrta2fl/fl;Emx1-Cre
Dmrta2fl/fl
Dmrta2fl/fl;Emx1-Cre
Tubb3
Eomes
Number of Tubb3+ cells
90
80
70
60
50
40
30
20
10
0
*
Dmrta2fl/fl
Dmrta2fl/fl;Emx1-Cre

Fig. 5

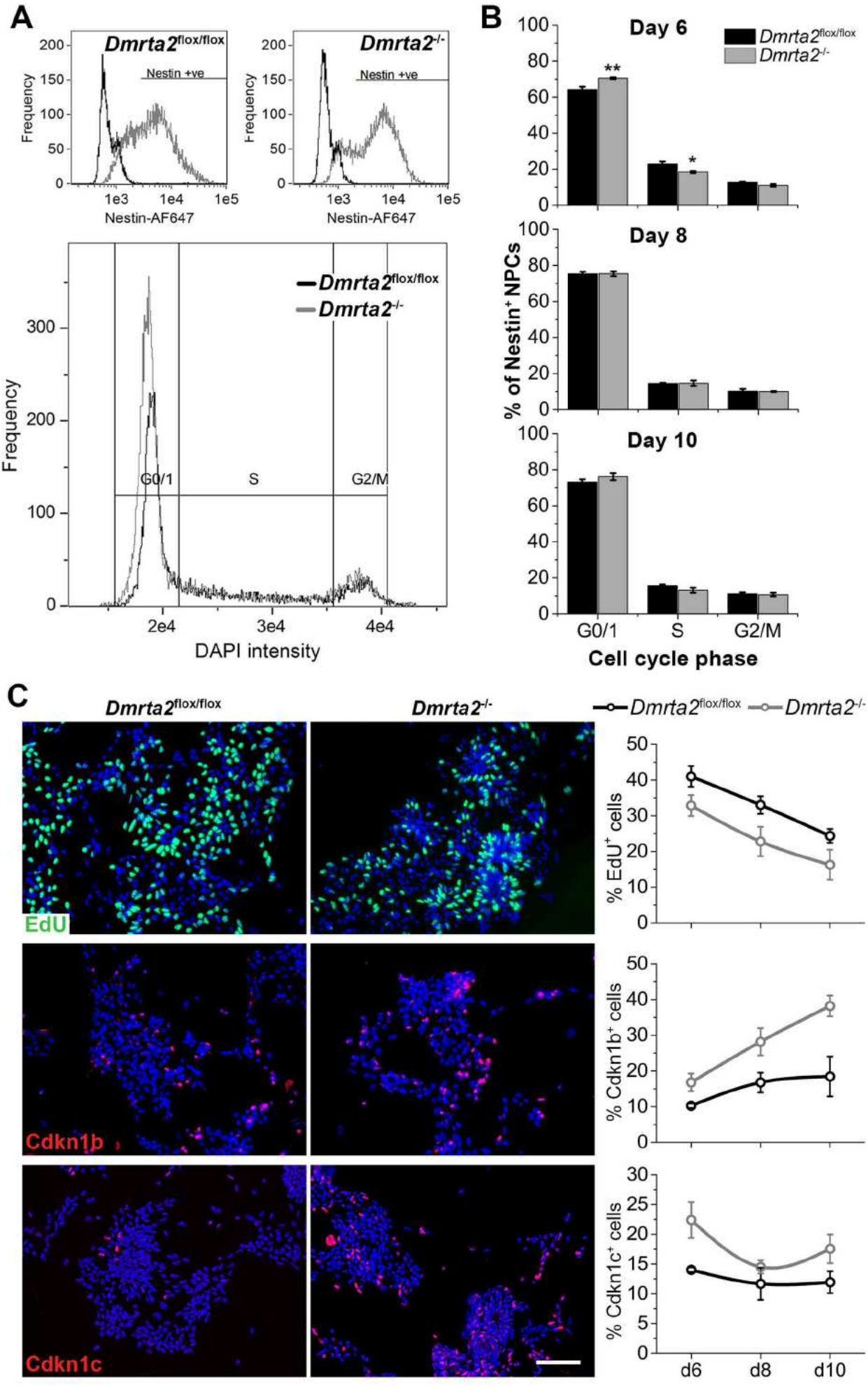
A
Dmrta2flox/flox
Dmrta2-/-
Nestin +ve
Frequency
Nestin-AF647
G0/1
S
G2/M
DAPI intensity
B
Day 6
Day 8
Day 10
% of Nestin+ NPCs
Cell cycle phase
C
EdU
Cdkn1b
Cdkn1c
% EdU+ cells
% Cdkn1b+ cells
% Cdkn1c+ cells
d6
d8
d10

Fig. 6

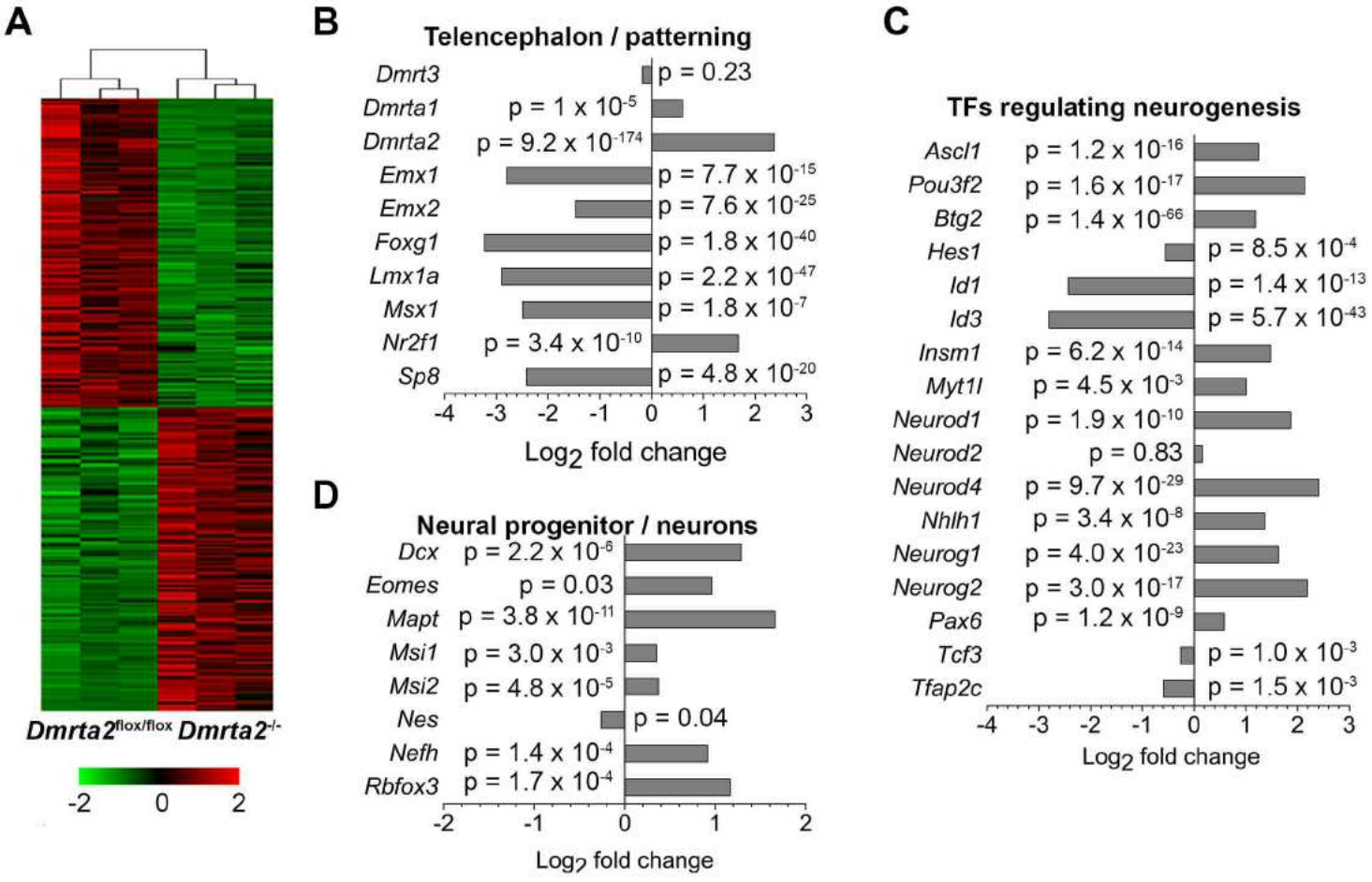
A
Dmrta2flox/flox Dmrta2-/-
-2
0
2
B
Telencephalon / patterning
Dmrt3
Dmrta1
Dmrta2
Emx1
Emx2
Foxg1
Lmx1a
Msx1
Nr2f1
Sp8
p = 0.23
p = 1 x 10-5
p = 9.2 x 10-174
p = 7.7 x 10-15
p = 7.6 x 10-25
p = 1.8 x 10-40
p = 2.2 x 10-47
p = 1.8 x 10-7
p = 3.4 x 10-10
p = 4.8 x 10-20
-4 -3 -2 -1 0 1 2 3
Log2 fold change
C
TFs regulating neurogenesis
Ascl1
Pou3f2
Btg2
Hes1
Id1
Id3
Insm1
Myt1l
Neurod1
Neurod2
Neurod4
Nhlh1
Neurog1
Neurog2
Pax6
Tcf3
Tfap2c
p = 1.2 x 10-16
p = 1.6 x 10-17
p = 1.4 x 10-66
p = 8.5 x 10-4
p = 1.4 x 10-13
p = 5.7 x 10-43
p = 6.2 x 10-14
p = 4.5 x 10-3
p = 1.9 x 10-10
p = 0.83
p = 9.7 x 10-29
p = 3.4 x 10-8
p = 4.0 x 10-23
p = 3.0 x 10-17
p = 1.2 x 10-9
p = 1.0 x 10-3
p = 1.5 x 10-3
-4 -3 -2 -1 0 1 2 3
Log2 fold change
D
Neural progenitor / neurons
Dcx
Eomes
Mapt
Msi1
Msi2
Nes
Nefh
Rbfox3
p = 2.2 x 10-6
p = 0.03
p = 3.8 x 10-11
p = 3.0 x 10-3
p = 4.8 x 10-5
p = 0.04
p = 1.4 x 10-4
p = 1.7 x 10-4
-2 -1 0 1 2
Log2 fold change

Fig. 7

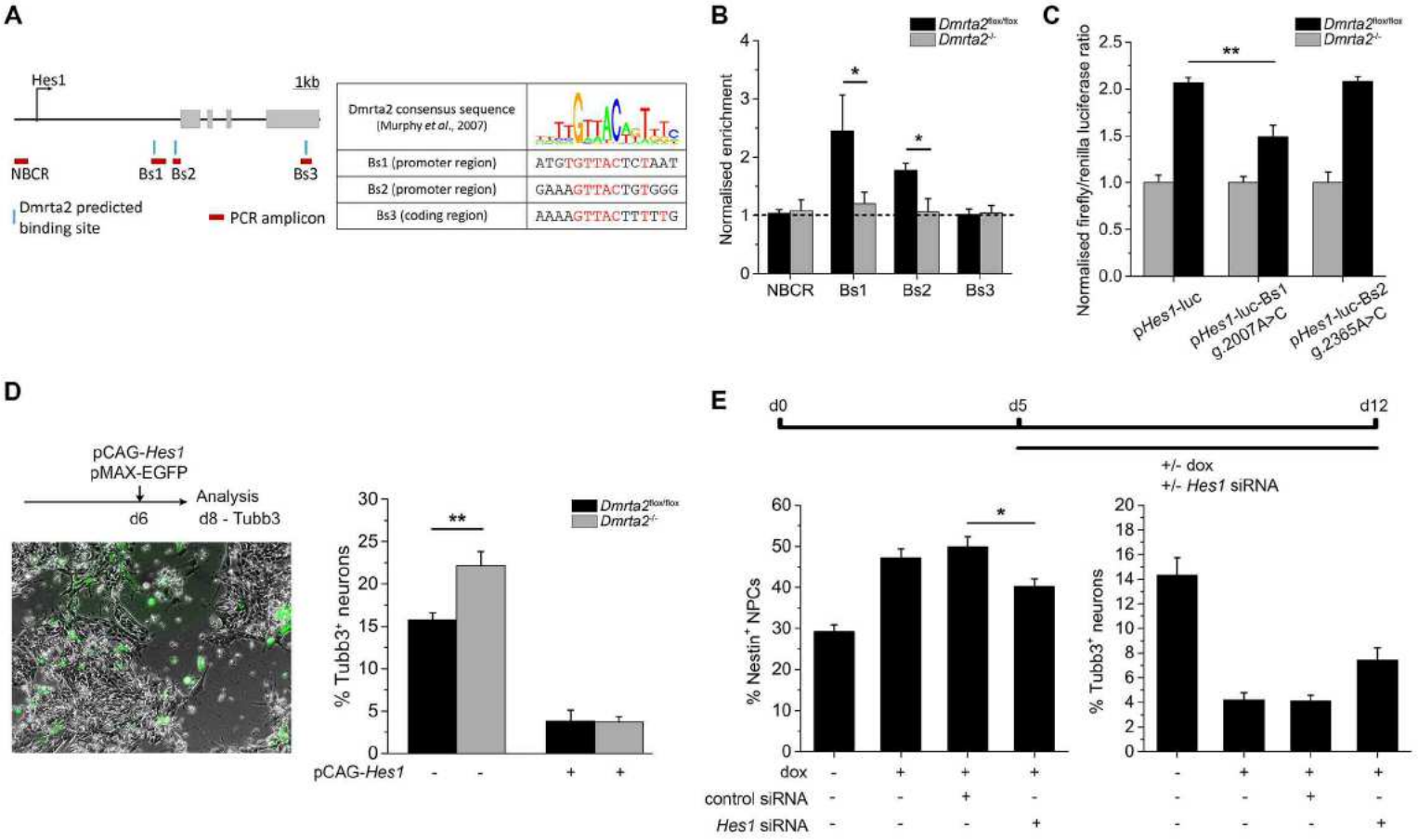
A
Hes1
1kb
NBCR
Bs1 Bs2
Bs3
Dmrta2 predicted binding site
PCR amplicon
Dmrta2 consensus sequence (Murphy et al., 2007)
Bs1 (promoter region) ATGTGTTACTC/TAAT
Bs2 (promoter region) GAAAGTTACTGTGGG
Bs3 (coding region) AAAAGTTACTTTTTG
B
Dmrta2flox/flox
Dmrta2-/-
Normalised enrichment
NBCR
Bs1
Bs2
Bs3
C
Normalised firefly/renilla luciferase ratio
pHes1-luc
pHes1-luc-Bs1 g.2007A>C
pHes1-luc-Bs2 g.2365A>C
D
pCAG-Hes1
pMAX-EGFP
d6
Analysis
d8 - Tubb3
% Tubb3+ neurons
pCAG-Hes1
E
d0
d5
d12
+/- dox
+/- Hes1 siRNA
% Nestin+ NPCs
% Tubb3+ neurons
dox
control siRNA
Hes1 siRNA

Fig. 8

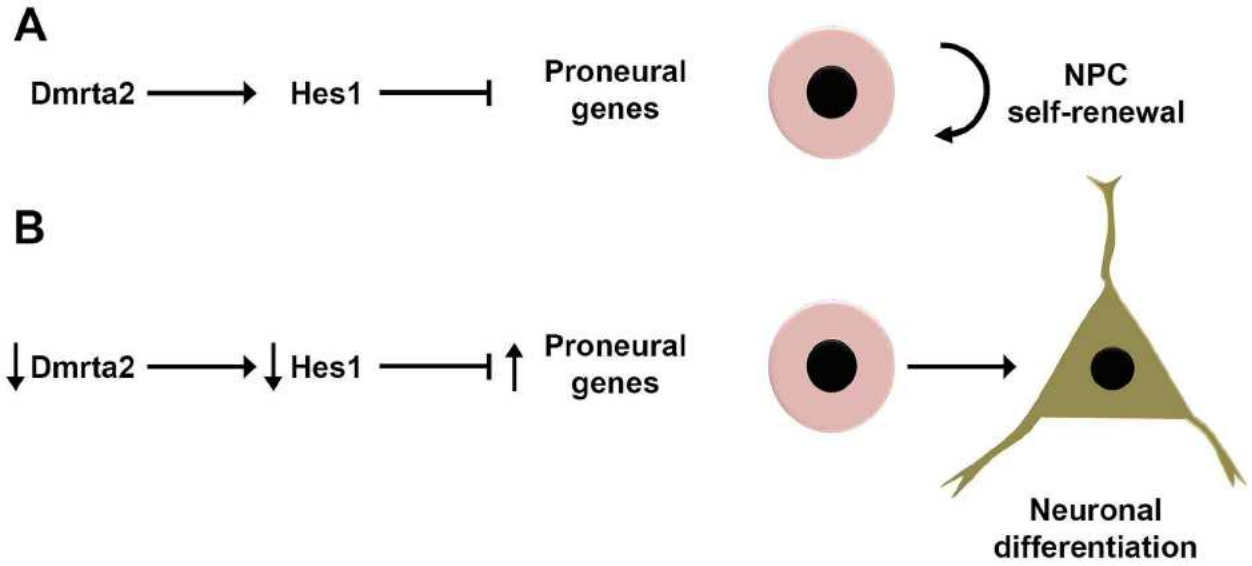
A
Dmrta2
Hes1
Proneural genes
NPC self-renewal
B
Dmrta2
Hes1
Proneural genes
Neuronal differentiation

SI Appendix

The Doublesex-related *Dmrta2* safeguards neural progenitor maintenance involving transcriptional regulation of *Hes1*

Author affilations

Fraser I. Young[1], Marc Keruzore[2#], Xinsheng Nan[3,#], Nicole Gennet[1], Eric J. Bellefroid[2‡], Meng Li[1,3‡]

1, Neuroscience and Mental Health Research Institute, School of Medicine, Cardiff University, Cardiff, CF24 4HQ, UK

2, Laboratoire de Génétique du Développement, Institut de Biologie et de MédecineMoléculaires, Université Libre de Bruxelles, Rue des Profs Jeener et Brachet, 126041 Gosselies, Belgium

3, School of Bioscience, Cardiff University, Cardiff, CF24 4HQ, UK

‡Corresponding authors: Meng Li, email: LiM26@cardiff.ac.uk Tel: +44-29-20688345; Eric Bellefroid, email: ebellefr@ulb.ac.be Tel: +32 26509732

SI Materials and Methods

Generation of *Dmrta2*$^{-/-}$ and *Dmrta2*$^{flox/flox}$ mESCs

The *Dmrta2* gene was targeted by homologous recombination using a *Dmrta2* targeting construct containing 5' and 3' arms for homologous recombination, a CMVhygrotkpA cassette flanked by two FRT sites for selection and subsequent removal of the selection cassette by flippase (Flp), exon 2 (E2) flanked by two loxP sites for Cre-mediated conditional knockout, and a Lox2272 site for facilitating exchange of reporters to the Dmrta2 locus (Fig S3*A*). Targeting was screened by southern blots for homologous recombination (Fig. S3*B*). In order to target the second *Dmrta2* allele, the CMVhygrotkpA cassette was removed from the first targeted *Dmrta2*^{mut} allele by transfection with Flp construct to result in *Dmrta2*^{flox}. The *Dmrta2*^{flox} allele was distinguished from wildtype *Dmrta2* by PCR genotyping using forward primer *Dmrta2*-KO7-p3f and reverse primer *Dmrta2*-KO7-p1r (Fig. S3*C* and Table S1). After targeting of the second *Dmrta2* allele, *Dmrta2*$^{flox/mut}$ mESCs were transfected with Flp construct to remove CMVhygrotkpA cassette from the second allele to generate control *Dmrta2*$^{flox/flox}$ mESCs. To generate *Dmrta2* null ES cells (*Dmrta2*$^{-/-}$), *Dmrta2*$^{flox/mut}$ cells were co-transfected with both Flp and Cre constructs to simultaneously remove CMVhygrotkpA cassette.

ESC differentiation

To differentiate ESCs towards a ventral telencephalic fate cells were seeded at 10 000 cells/cm^2 in gelatin-coated 6 well plates and cultured in N2B27 medium. Differentiation medium was supplemented with 100 nM LDN193189, 10 µM SB431542 from days 0 to 4, 1 µM XAV939 from day 0 to 6, and 1 µg/ml SHH and 10nM SAG (all Tocris) between days 2 and 10 (Sigma-Aldrich). To obtain a more caudal phenotype ESCs were seeded at 10 000 cells/cm^2 in gelatin-coated 6 well plates and cultured in N2B27 supplemented with 100 nM LDN193189 and 10 µM SB431542 from days 0 to 4. Between days 2 and 6 of differentiation N2B27 prepared with B27 supplement containing vitamin A was used. ESCs were differentiated towards a ventral midbrain fate as described previously (23). Briefly, ESCs were seeded at 2 500 cells/cm^2 in gelatin-coated 6 well plates and cultured in N2B27 medium. Differentiation medium was supplemented with PD0325901 from day 2 to 4 and 100 ng/ml SHH, 1 µM Purmorphamine (all Tocris) and 100 ng/ml Fgf-8 between days 7 and 11. On day 5 of differentiation neural progenitor cells were dissociated using Trypsin/EDTA and replated onto poly-D-lysine/laminin coated surface at a density of 50,000 cells/cm^2 for neuronal differentiation and maturation.

Primary antibodies

The primary antibodies used are: rat anti-Bcl11b (Abcam, ab18465, 1:500), mouse anti-Coup-TF1 (Perseus Proteomics, PP-H8132-00, 1:200), custom rabbit anti-Dmrta2 (1:2000), custom guinea pig anti-Dmrta2 (1:2000), rabbit anti-Eomes (Abcam, ab23345, 1:500), mouse anti-FORSE-1 (Developmental Studies Hybridoma Bank (DSHB, 1:500), goat anti-FoxA2 (Santa Cruz, sc6554, 1:100), mouse anti-Gad65/67 (Merck Millipore, Mab5406, 1:500), mouse anti-GFP (Thermofisher Scientific, A11120, 1:200), rabbit anti-Ki67 (Novocastro, NCL-Ki67p, 1:500), mouse anti-Lim1 (DSHB, 1:10), custom guinea pig anti-Lmx1a (1:1000), rabbit anti-Musashi1 (Merck Millipore, AB5977, 1:200), chicken anti-Nestin (Neuromics, CH23001, 1:500), mouse anti-NeuN (Merck Millipore, MAB377, 1:400), rabbit anti-Nkx2.1 (Abcam, ab40880, 1:1000), rabbit anti-Nurr1 (Santa Cruz, sc990, 1:200), goat anti-Olig2 (R&D Systems, AF2418, 1:200), goat anti-Otx2 (Santa Cruz, sc30659, 1:100), mouse anti-Pax6 (DSHB, 1:1000), rabbit anti-p27^{kip1} (Santa Cruz, sc528, 1:200), rabbit anti-p57^{kip2} (Abcam, ab4058, 1:250), mouse anti-SatB2 (Abcam, ab51502, 1:10), rabbit anti-

Tbr1 (Abcam, ab31940, 1:1000), sheep anti-Tyrosine Hydroxylase (Pel-Freez, P60101/1, 1:500), rabbit anti-TUBB3 (Covance, PRB-435p, 1:1000), rabbit anti-Tubb3 (Sigma, T2200, 1:200) and mouse anti-vGlut1 (Merck Millipore, MAB5502, 1:500).

SI figure legends

Fig. S1. ESC differentiation produces highly homogenous cultures of cortical NPCs and neurons. (*A*) Schematic representation of alternative differentiation protocols used to derive NPCs and neurons of ventral telencephalic, ventral midbrain and more caudal identities. (*B*) Additional characterisation data confirming Dmrta2 expression is restricted to telencephalic NPCs of dorsal, but not ventral, identity as demonstrated by co-localisation with Coup-TF1 but not Nkx2.1. (*C)* Additional characterisation data demonstrating the absence of FoxA2 staining in cortical NPC cultures. (*D*) Additional immunostaining data demonstrating the co-localisation of Dmrta2 with Otx2 in cortical NPC cultures. (*E*-*G*) Additional characterisation data confirming a glutamatergic phenotype of neurons derived from cortical NPC cultures demonstrated by positive immunostaining for Bcl11b and vGlut1, and an absence of staining for GAD65/67 (*E*), Th and Nurr1 (*F*), and Isl1 and Olig2 (*G*). All scale bars, 100 µm.

Fig. S2. Transgenic expression of *Dmrta2* does not compromise NPC neurogenic competence. (*A*) Experimental scheme. Monolayer cultures of *Dmrta2*-ESCs were exposed to doxycycline or vehicle control from day 5 to 9. Cultures were harvested at days 7, 9 and 14 for qPCR and at day 14 for immunocytochemistry. (*B*) Phase contrast image of day 14 cultures treated with vehicle or doxycycline between day 5-9, showing similar neuronal content. (*C*) Tubb3 antibody staining of day 14 sister cultures. (*D*) qPCR for *Tubb3* demonstrating the recovery of *Tubb3* expression levels at day 14 in doxycycline-treated cultures compared to control cultures.

Fig. S3. Generation and validation of *Dmrta2*$^{flox/flox}$ and *Dmrta2*$^{-/-}$ mESC lines**.**
(*A*) The *Dmrta2* gene was targeted by homologous recombination using a *Dmrta2* targeting construct containing 5' and 3' arms for homologous recombination. (*B*) Targeting was screened by Southern Blots for 5' and 3' homologous recombination. ScaI digestion generated a 8.1 kb fragment in wt and an 11.29 kb fragment in *Dmrta2*^{mut} ESC cells detected with 5' probe. SacI digestion generated a 10.1 kb fragment in wt and an 8.88 kb fragment in *Dmrta2*^{mut} ES cells detected with 3' probe (not shown). (*C*) *Dmrta2*^{flox} alleles were distinguished from wildtype *Dmrta2* by PCR to generate 479bp and 365bp fragments, respectively. (*D*) Corresponding images of Pax6 and Dmrta2 immunostaining of *Dmrta2*$^{flox/flox}$ and *Dmrta2*$^{-/-}$ neural progenitor cells on day 8 of differentiation, confirming knockout of *Dmrta2* protein. Scale bar: 100 µm

Fig. S4. Enforced expression of *Dmrta2* transgene keeps cortical NPCs in the cell cycle**.** (*A*) Experimental scheme. Monolayer cultures of *Dmrta2*-ESCs were exposed to doxycycline or vehicle control from day 5 to 12. Cultures were harvested every day from day 6 till 12 and samples processed for qPCR. (*B*) qPCR analysis of *Cdkn1b* and *Cdkn1c* from day 6-12. Levels of mRNA expression were normalised to day 5. Error bars indicate means ± s.e.m. of three biological replicates. (*C*) Day 12 cultures treated with doxycycline (middle) or vehicle (left) from day 5 were stained with antibodies against Ki67 (red) and counter stained with DAPI (blue), and quantification of Ki67^{+} cells. Scale bar: 100µm.

Fig. S5. Extended RNAseq data. (*A, B*) Top 10 enriched gene ontology terms for biological processes associated with transcripts identified as upregulated (*A*) or downregulated (*B*) in *Dmrta2*$^{-/-}$ NPCs relative to *Dmrta2*$^{flox/flox}$ NPCs. Differentially regulated transcripts used for this analysis were restricted to those with an adjusted p-value<0.01 and a fold change greater than two-fold. Modified Fisher's exact p-value and Benjamini-Hochberg correction for multiple comparisons. (*C*) Top 15 transcripts identified as upregulated or downregulated in by *Dmrta2*$^{-/-}$ NPCs relative to *Dmrta2*$^{flox/flox}$ NPCs.

Supplementary table 1 – Primers used in PCR and qPCR

Gene	F primer (5'→3')	R primer (5'→3')	Size (bp)
Dmrt5 genotyping - p1r	GGACCTGCCCCCTAACAAGAGTA	-	-
Dmrt5 genotyping - p3f	CGCGGCCTGCCTACGAAGTCTTTG	-	-
Dmrt5 genotyping - p4f	GGGGTGGGGGCGTACTTGTTTACAG	-	-
Cyclophillin	GGCAAATGCTGGACCAAACAC	TTCCTGGACCCAAAACGCTC	147
Dmrt5	GCCTGCCTACGAAGTCTTTGGCTCGGTTT	CGTCTTGGGAAACAGATCAAACTTCTGCAATTT	136
GAPDH	AGGTCGGTGTGAACGGATTTG	ACTGTGCCGTTGAATTTGCC	166
Hes1	TCGGTGGGTCCTAACGCAGT	ACGGGTAGCAGTGGCCTGAG	105
HMBS	ACTGGTGGAGTCTGGAGTCTAGATGGC	GCCAGGCTGATGCCCAGGTT	181
Map2	CTGGACATCAGCCTCACTCA	AATAGGTGCCCTGTGACCTG	163
Neurod1	CATGAGCGAGTCATGAGTGC	GCACAGTGGATTCGTTTCCC	92
Neurod4	AGGCCAATGCTAGAGAACGG	TCCTTGCCAGTCGAAGAGTC	129
Neurog2	GCTGTGGGAATTTCACCTGT	AAATTTCCACGCTTGCATTC	236
Cdkn1b	ACGCCAGACGTAAACAGCTC	GAGGCAGATGGTTTAAGAGTGC	192
Cdkn1c	GAGGAGCAGGACGAGAATCA	CACGTTTGGAGAGGGACACC	198
Eomes	GAGAAAGCGCCTGTCTCCCA	CCCATGCCTTTGGAGGTGTC	108
Tubb3	ATCAGCAAGGTGCGTGAGGAG	ATGGACAGGGTGGCGTTGTAG	113
ChIP - NBCR	AGGACATCAGGTTCTGTGCC	AGATTCCCCACAAGATTCCC	240
ChIP - Bs1	ACATACAGAGTTCGAGCGGG	TTCTCTGGGCTTTGCTTAG	235
ChIP - Bs2	CGTGTCTCTTCCTCCCATTG	ATTCCGCTGTTATCAGCACC	155
ChIP - Bs3	CCACCTCTCTCTTCTGACGG	AGGCGCAATCCAATATGAAC	184

Fig. S1

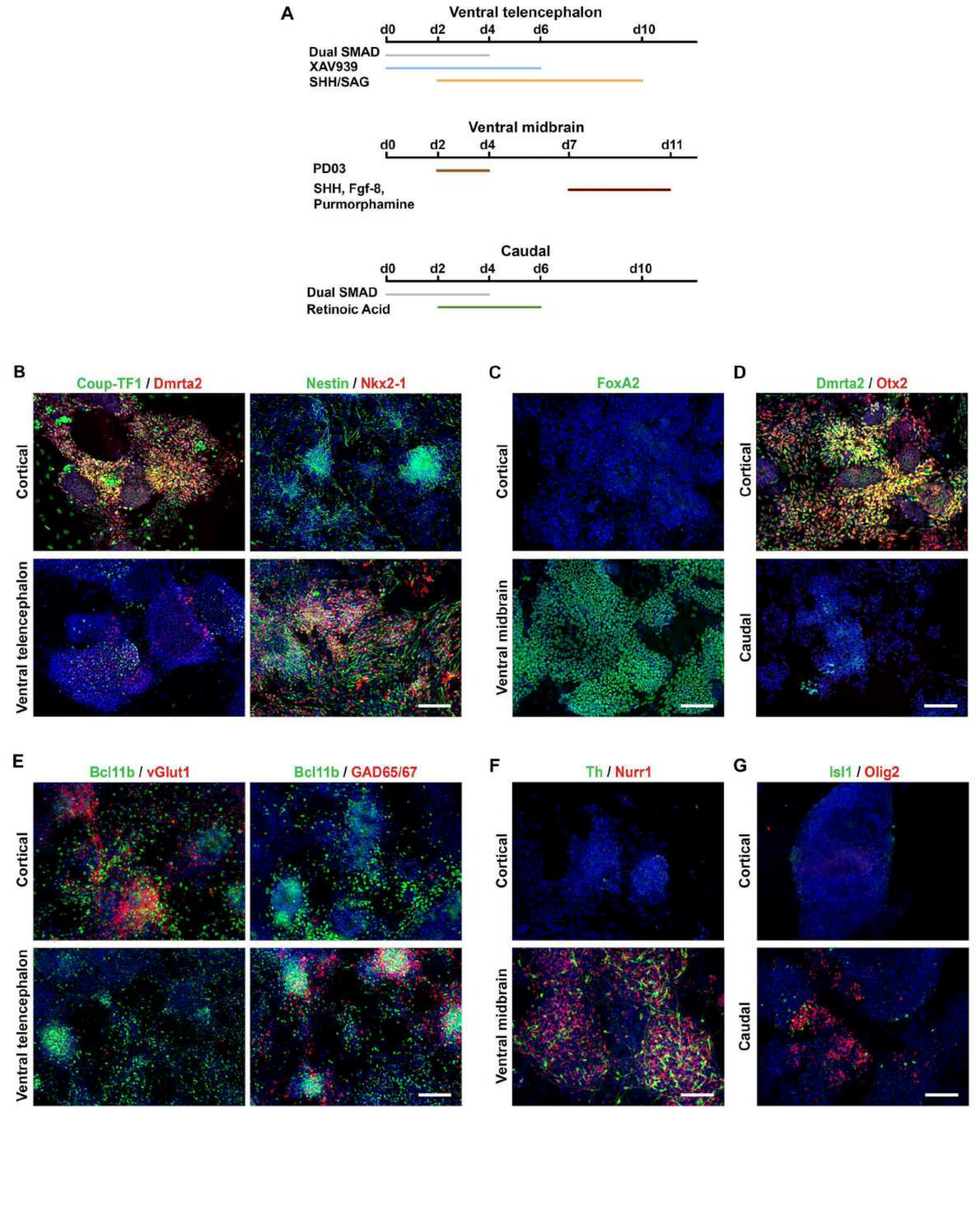
A
Ventral telencephalon
d0
d2
d4
d6
d10
Dual SMAD
XAV939
SHH/SAG
Ventral midbrain
d0
d2
d4
d7
d11
PD03
SHH, Fgf-8,
Purmorphamine
Caudal
d0
d2
d4
d6
d10
Dual SMAD
Retinoic Acid
B
Coup-TF1 / Dmrta2
Nestin / Nkx2-1
Cortical
Ventral telencephalon
C
FoxA2
Cortical
Ventral midbrain
D
Dmrta2 / Otx2
Cortical
Caudal
E
Bcl11b / vGlut1
Bcl11b / GAD65/67
Cortical
Ventral telencephalon
F
Th / Nurr1
Cortical
Ventral midbrain
G
Isl1 / Olig2
Cortical
Caudal

Fig. S2

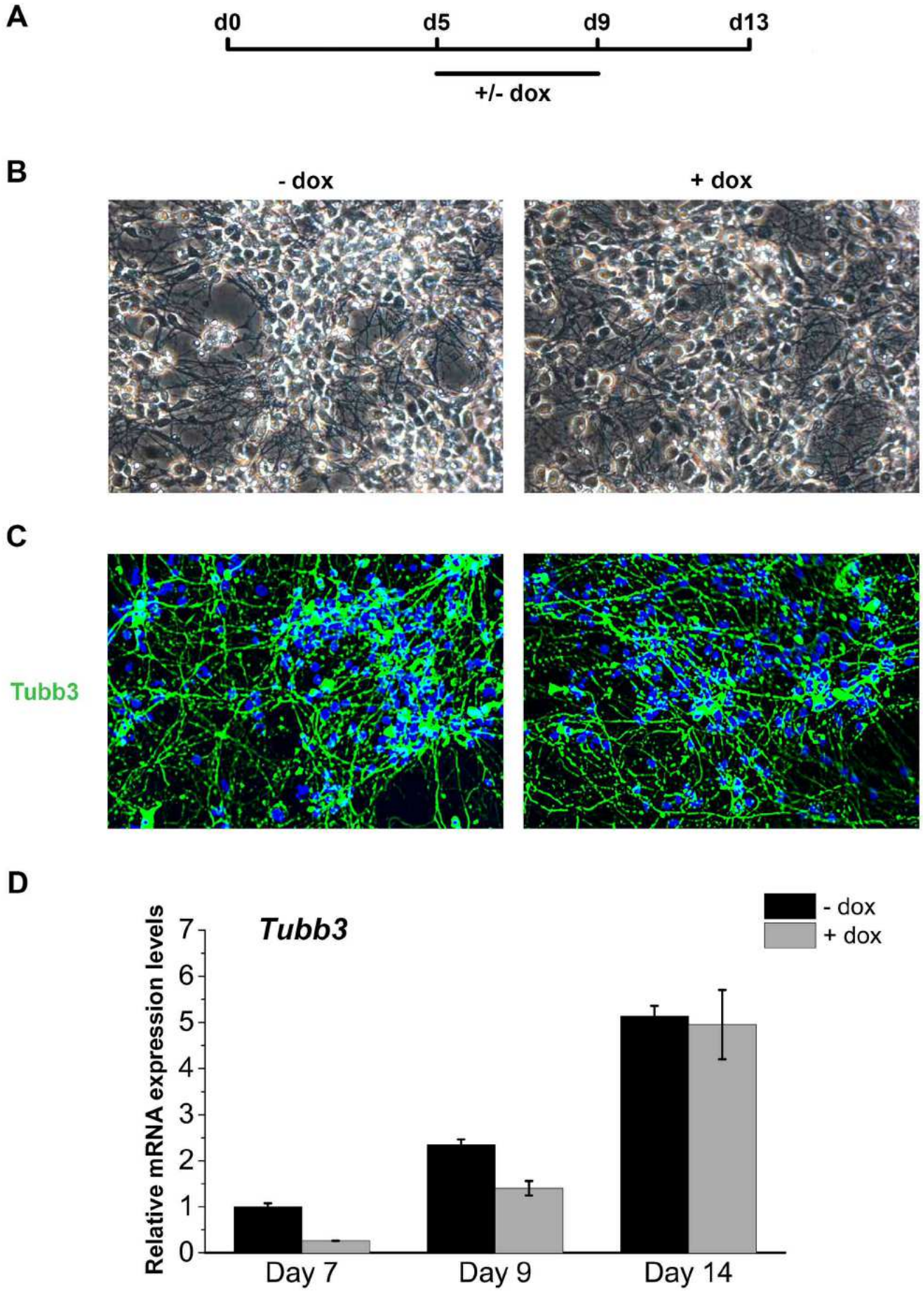
A
d0
d5
d9
d13
+/- dox
B
- dox
+ dox
C
Tubb3
D
Tubb3
- dox
+ dox
Relative mRNA expression levels
0
1
2
3
4
5
6
7
Day 7
Day 9
Day 14

Fig. S3

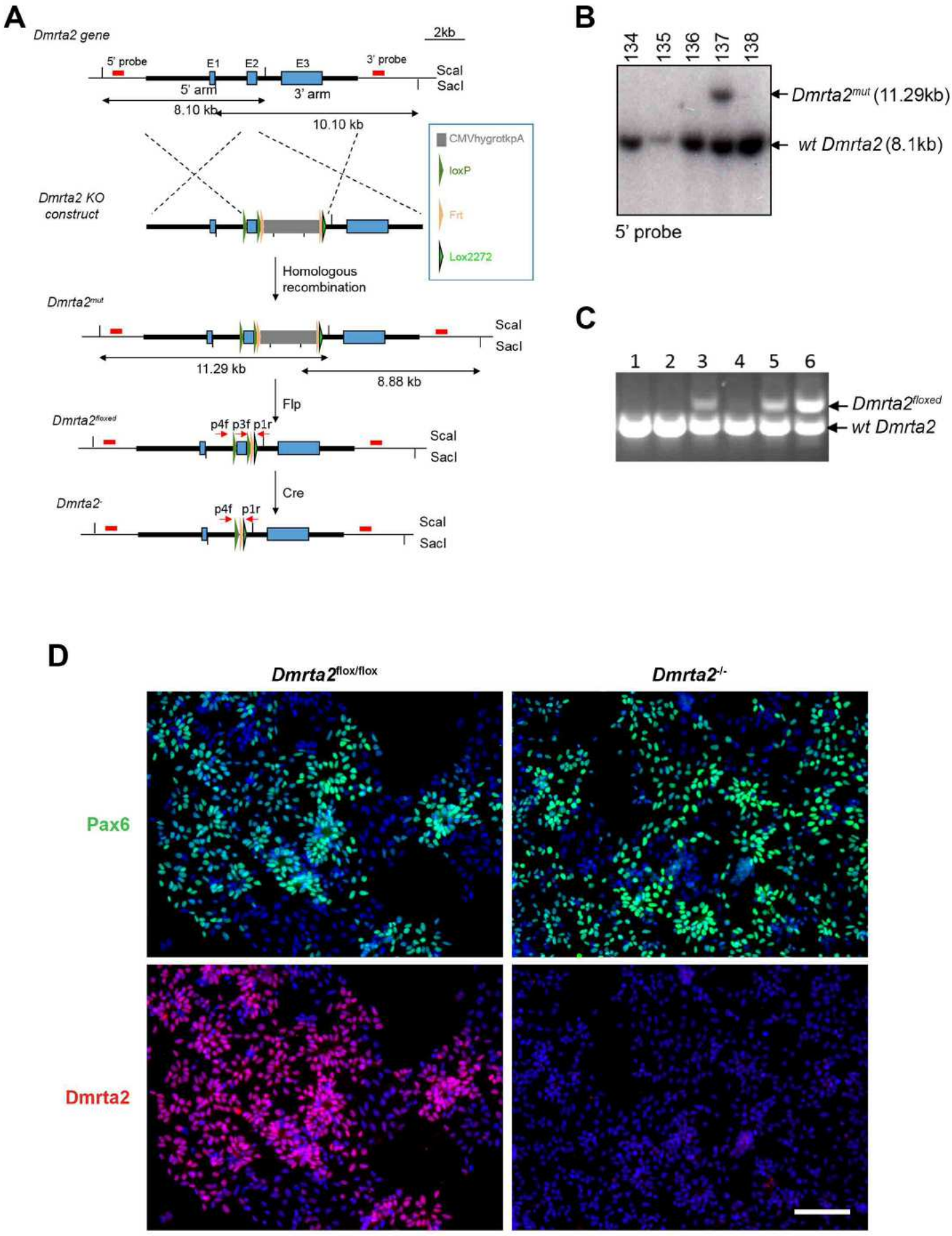
A
Dmrta2 gene
2kb
5' probe
E1
E2
E3
3' probe
ScaI
SacI
5' arm
3' arm
8.10 kb
10.10 kb
CMVhygrotkpA
loxP
Frt
Lox2272
Dmrta2 KO construct
Homologous recombination
Dmrta2mut
11.29 kb
8.88 kb
Flp
Dmrta2floxed
p4f p3f p1r
Cre
Dmrta2-
p4f p1r
B
134
135
136
137
138
Dmrta2mut (11.29kb)
wt Dmrta2 (8.1kb)
5' probe
C
1 2 3 4 5 6
Dmrta2floxed
wt Dmrta2
D
Dmrta2flox/flox
Dmrta2-/-
Pax6
Dmrta2

Fig. S4

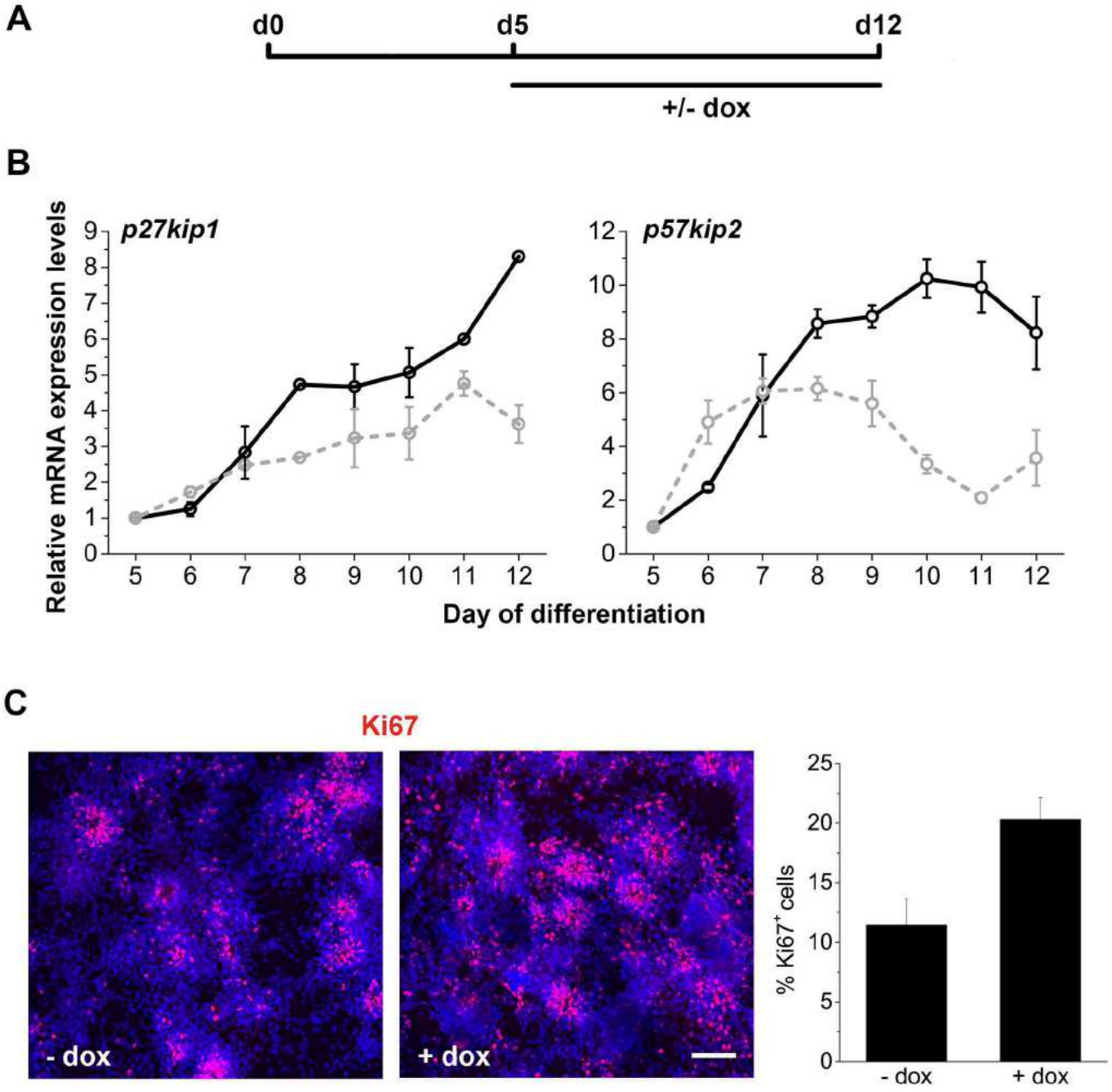
A
d0
d5
d12
+/- dox
B
p27kip1
p57kip2
Relative mRNA expression levels
Day of differentiation
C
Ki67
- dox
+ dox
% Ki67+ cells

Fig. S5

A

Top 10 enriched GO terms associated with upregulated transcripts (650 genes)

GO term		Gene count	p-value	Benjamini correction
Nervous system development	GO:0007399	151	2.17×10^{-27}	1.14×10^{-23}
Generation of neurons	GO:0048699	115	1.17×10^{-22}	3.01×10^{-19}
Neuron differentiation	GO:0030182	106	1.16×10^{-21}	1.52×10^{-18}
Neurogenesis	GO:0022008	118	6.19×10^{-22}	1.09×10^{-18}
Regulation of nervous system development	GO:0051960	82	3.82×10^{-20}	4.03×10^{-17}
Cell-cell signalling	GO:0007267	83	1.19×10^{-19}	1.05×10^{-16}
Regulation of neurogenesis	GO:0050767	71	7.2×10^{-17}	6.51×10^{-14}
Synaptic transmission	GO:0007268	56	4.49×10^{-17}	2.96×10^{-14}
Neuron development	GO:0048666	85	1.53×10^{-17}	1.15×10^{-14}
Regulation of multicellular organismal development	GO:2000026	116	1.67×10^{-15}	8.78×10^{-13}

B

Top 10 enriched GO terms associated with downregulated transcripts (936 genes)

GO term		Gene count	p-value	Benjamini correction
Biological adhesion	GO:0022611	159	3.35×10^{-31}	2.25×10^{-27}
Cell adhesion	GO:0007155	155	1.55×10^{-29}	5.2×10^{-26}
Organ morphogenesis	GO:009887	129	2.86×10^{-28}	6.4×10^{-25}
Epithelium development	GO:0060429	131	5.31×10^{-25}	8.92×10^{-22}
Regulation of multicellular organismal development	GO:2000026	177	6.92×10^{-24}	7.75×10^{-21}
Locomotion	GO:0040011	157	5.2×10^{-24}	6.98×10^{-21}
Cell proliferation	GO:0008283	169	8.98×10^{-23}	7.54×10^{-20}
Regulation of cell proliferation	GO:0042127	156	1.57×10^{-23}	1.5×10^{-20}
Tissue morphogenesis	GO:0048729	92	7.6×10^{-22}	5.67×10^{-19}
Skeletal system development	GO:0001501	76	2.17×10^{-21}	1.46×10^{-18}

C

Top 15 transcripts upregulated in Dmrt5$^{-/-}$ NPCs

Gene	Description	Adj p-value	Fold change
Plagl1	pleiomorphic adenoma gene-like 1	2.86×10^{-207}	23.10404
Dmrta2	doublesex and mab-3 related transcription factor like family A2	9.15×10^{-174}	5.196742
Adamtsl1	ADAMTS-like 1	9.35×10^{-124}	12.43845
Sfrp2	secreted frizzled-related protein 2	3.63×10^{-82}	5.232482
Shh	sonic hedgehog	5.15×10^{-72}	17.39337
Btg2	B cell translocation gene 2, anti-proliferative	1.39×10^{-68}	2.272523
Meis1	Meis homeobox 1	2.32×10^{-64}	3.415617
Abcd2	ATP-binding cassette, sub-family D (ALD), member 2	7.23×10^{-62}	6.451097
Fat4	FAT atypical cadherin 4	3×10^{-61}	3.724901
Ednrb	endothelin receptor type B	3.26×10^{-59}	6.364833
Glyctk	glycerate kinase	3.35×10^{-52}	3.14408
Nt5c	5',3'-nucleotidase, cytosolic	2.39×10^{-51}	3.82449
Nts	neurotensin	1.04×10^{-46}	9.425834
Nap1l5	nucleosome assembly protein 1-like 5	1.64×10^{-41}	17.80717
Cdc42ep4	CDC42 effector protein (Rho GTPase binding) 4	1.08×10^{-40}	2.620299

Top 15 transcripts downregulated in Dmrt5$^{-/-}$ NPCs

Gene	Description	Adj p-value	Fold change
Pde1a	phosphodiesterase 1A, calmodulin-dependent	2.07×10^{-94}	-12.007
Vnn1	vanin 1	9.7×10^{-76}	-9.72749
Epha4	Eph receptor A4	5.78×10^{-68}	-2.67969
Igf2r	insulin-like growth factor 2 receptor	2.19×10^{-62}	-6.44116
Fblim1	filamin binding LIM protein 1	4.02×10^{-61}	-4.08388
Sema3c	sema domain, immunoglobulin domain (Ig), short basic domain, secreted, (semaphorin) 3C	2.74×10^{-55}	-11.04
Klhl9	kelch-like 9	4.08×10^{-54}	-4.08125
Fam46c	family with sequence similarity 46, member C	6.38×10^{-54}	-4.87465
Pax2	paired box 2	1.11×10^{-52}	-11.1797
Tll2	tolloid-like 2	2.11×10^{-50}	-11.2469
Grb10	growth factor receptor bound protein 10	1.74×10^{-48}	-10.3381
Lmx1a	LIM homeobox transcription factor 1 alpha	2.23×10^{-47}	-7.43055
Slc16a2	solute carrier family 16 (monocarboxylic acid transporters), member 2	2.21×10^{-46}	-4.99957
Gadd45b	growth arrest and DNA-damage-inducible 45 beta	3.18×10^{-46}	-9.56437
Cachd1	cache domain containing 1	8.3×10^{-45}	-2.15865